

# Large- $N$ dynamics of dimensionally reduced 4D $SU(N)$ super Yang-Mills theory

**Jan Ambjørn and Jun Nishimura\***

*Niels Bohr Institute, Copenhagen University  
Blegdamsvej 17, DK-2100 Copenhagen Ø, Denmark  
E-mail: ambjorn@nbi.dk, nisimura@nbi.dk*

**Konstantinos N. Anagnostopoulos**

*Department of Physics, University of Crete  
P.O. Box 2208, GR-71003 Heraklion, Greece  
E-mail: konstant@kirsitsis.physics.uoc.gr*

**Wolfgang Bietenholz**

*NORDITA Blegdamsvej 17, DK-2100 Copenhagen Ø, Denmark  
E-mail: bietenho@nordita.dk*

**Tomohiro Hotta**

*Institute of Physics, University of Tokyo  
Komaba, Meguro-ku, Tokyo 153-8902, Japan  
E-mail: hotta@hep1.c.u-tokyo.ac.jp*

**ABSTRACT:** We perform Monte Carlo simulations of a supersymmetric matrix model, which is obtained by dimensional reduction of 4D  $SU(N)$  super Yang-Mills theory. The model can be considered as a four-dimensional counterpart of the IIB matrix model. We extract the space-time structure represented by the eigenvalues of bosonic matrices. In particular we compare the large- $N$  behavior of the space-time extent with the result obtained from a low-energy effective theory. We measure various Wilson loop correlators which represent string amplitudes and we observe a non-trivial universal scaling in  $N$ . We also observe that the Eguchi-Kawai equivalence to ordinary gauge theory does hold at least within a finite range of scale. Comparison with the results for the bosonic case clarifies the rôle of supersymmetry in the large- $N$  dynamics. It does affect the multi-point correlators qualitatively, but the Eguchi-Kawai equivalence is observed even in the bosonic case.

**KEYWORDS:** Superstrings and Heterotic Strings, Supersymmetry and Duality, Matrix Models, Nonperturbative Effects.

---

\*Permanent address: Department of Physics, Nagoya University, Nagoya 464-8602, Japan.

---

## Contents

|   |           |
|---|-----------|
| <b>1. Introduction</b>                              | <b>1</b>  |
| <b>2. The model</b>                                 | <b>4</b>  |
| <b>3. The space-time structure</b>                  | <b>6</b>  |
| <b>4. Wilson loop correlation functions</b>         | <b>10</b> |
| 4.1 One-point function and Eguchi-Kawai equivalence | 11        |
| 4.2 Multi-point functions and universal scaling     | 14        |
| 4.3 Interpretation of the large- $N$ scaling        | 17        |
| <b>5. Summary and discussion</b>                    | <b>21</b> |
| A. The algorithm for the Monte Carlo simulation     | 23        |
| B. Results for the bosonic case                     | 28        |

---

### 1. Introduction

A recent excitement in string theory is that we finally arrive at concrete proposals for non-perturbative definitions of superstring theory [1]–[4]. In particular, Matrix Theory [1] and the IIB matrix model [2], which are candidates for a non-perturbative definition of M-theory and type-IIB superstring theory, respectively, have attracted considerable interest (for reviews, see refs. [5, 6]). The proposed formulations take the form of large- $N$  reduced models [7], which can be obtained by dimensional reduction of large- $N$  gauge theories; a reduction to one dimension for M-theory, and to zero dimension (one point) for type-IIB superstring theory. These proposals are supported by some evidences such as the similarity of the hamiltonian (or the action) to that of membranes or strings, the appearance of soliton-type objects known as D-branes with consistent interactions, and the consistency with string dualities upon compactification. For the IIB matrix model, even an attempt to establish a direct

connection to perturbative string theory has been made by deriving the light-cone string field hamiltonian from loop equations of the model [8]. This attempt was indeed successful, albeit with the aid of symmetry and power-counting arguments. Further variants of that model have been proposed in refs. [9].

As another approach to analyze these proposals we can investigate the dynamical properties of large- $N$  reduced models of this kind, and verify if they really have the potential to describe non-perturbative string theory. In ref. [10] a two-dimensional reduced model with unitary matrices has been studied in this context. There, a large- $N$  limit, which differs from the planar limit (or 't Hooft limit), has been discovered numerically.<sup>1</sup> A hermitean matrix model obtained by simply omitting the fermions in the IIB matrix model, and its generalizations to arbitrary dimensions larger than two, have been studied in refs. [12, 13]. In ref. [13], Monte Carlo simulations up to  $N = 256$  have been reported and analytical methods such as perturbation theory, Schwinger-Dyson equations and  $1/D$  expansions have been applied, providing a comprehensive understanding of the large- $N$  dynamics of that model. A new type of Monte Carlo technique was used to extract the value of the partition function [14, 12]. This technique has been further applied to extract the asymptotic behavior of the eigenvalue distribution for large eigenvalues [15, 16].

In the present paper, we make a first attempt to extract the large- $N$  dynamics of a *supersymmetric large- $N$  reduced model* obtained by dimensional reduction of 4D supersymmetric Yang-Mills theory. The model can be regarded as a 4D counterpart of the IIB matrix model. The bosonic model is well understood [12, 13], but the inclusion of fermions makes the system far more complicated. An attempt to study the model analytically maps it onto a soluble system [17], but the relevance to the original model is unclear due to a non-trivial change of variables in an analytic continuation. Here we take a direct approach, based on Monte Carlo simulations. Fermions are completely included by the use of the so-called Hybrid-R algorithm [18], which is one of the standard methods in QCD simulations with dynamical quarks.

One of the features that makes the IIB matrix model most attractive as a non-perturbative definition of string theory is that space-time is dynamically generated as the eigenvalue distribution of the bosonic matrices [2, 19, 20]. In ref. [19] a low-energy effective theory of the model is constructed, where the authors discuss some possible mechanisms that may induce a collapse of the eigenvalue distribution to a four-dimensional manifold. We extract the large- $N$  behavior of the space-time extent in our model and compare the result with the prediction obtained by the low-energy effective theory. Another dynamical issue to be addressed in this context is the space-time uncertainty relation, which was proposed as a principle for con-

---

<sup>1</sup>This non-planar large- $N$  limit has recently been re-interpreted as a continuum limit of non-commutative gauge theory [11].

structing non-perturbative string theory [21]. We extract the large- $N$  behavior of the space-time uncertainty of our model and confirm that the model indeed satisfies the proposed principle.

Another attractive feature of the IIB matrix model as a non-perturbative definition of string theory is that its only parameter  $g$  is a simple scale parameter.<sup>2</sup> One has to tune  $g$  suitably as one sends  $N$  to infinity, so that the correlation functions have finite large- $N$  limits. According to ref. [8], Wilson loop operators can be interpreted as the string creation and annihilation operators, and it was found that  $g^2 N$  should be fixed in order to obtain the light-cone string field hamiltonian in the large- $N$  limit. It is a non-trivial test of the model to verify if the correlation functions of Wilson loops really have a universal large- $N$  scaling. We address this issue in the present model and show that there is indeed a universal large- $N$  scaling at fixed  $g^2 N$ .

We also address yet another important dynamical issue in this model, namely the question of equivalence to ordinary super Yang-Mills theory in the sense of Eguchi and Kawai [7], which is exactly the way large- $N$  reduced models first appeared in history. The crucial observation is that large- $N$  gauge theory does not depend on the volume (under some assumptions), which inspired Eguchi and Kawai to propose the zero-volume limit of large- $N$  gauge theory as a model equivalent to the gauge theories in an infinite volume [7]. One of the assumptions is that the  $(\mathbb{Z}_N)^D$  symmetry of the model is *not* spontaneously broken, where  $D$  is the space-time dimension. However, in the purely bosonic case in  $D > 2$ , the symmetry *is* spontaneously broken at weak coupling [22], thus preventing one from taking a continuum limit. This led to modifications of the model [22]–[26] so that the  $(\mathbb{Z}_N)^D$  symmetry is not spontaneously broken while keeping the equivalence valid. In the supersymmetric case, the effective action which induces the spontaneous symmetry breaking of the  $(\mathbb{Z}_N)^D$  symmetry is naively cancelled by the contributions of fermions. Indeed, in the scalar field case, it has been shown that the reduced model is equivalent to the field theory without such modifications [27]. We observe in the present supersymmetric model that the Eguchi-Kawai equivalence indeed holds at least in a finite range of scale. What is rather remarkable is that actually this is true also for the bosonic case, which is contrary to what has been expected.

In section 2 we describe the model we are going to investigate. In section 3 we study the space-time structure of the model. In section 4 we present our results for correlation functions of Wilson loop and Polyakov line operators, and we discuss the Eguchi-Kawai equivalence as well as the universal scaling behavior. Section 5 is devoted to a summary and discussion. In appendix A we comment on the algorithm we used for the simulation. In appendix B we present the corresponding results for the bosonic case for comparison.

---

<sup>2</sup>This means in particular that the string coupling constant, which is related to the vacuum expectation value of the dilaton field, is *not* a tunable parameter. We come back to this point in section 4.3.

## 2. The model

The model we investigate is a supersymmetric matrix model obtained by dimensional reduction of 4D  $SU(N)$  super Yang-Mills theory. The partition function is given by

$$\begin{aligned} Z &= \int dA e^{-S_b} \int d\psi d\bar{\psi} e^{-S_f}, \quad S_b = -\frac{1}{4g^2} \text{tr}[A_\mu, A_\nu]^2, \\ S_f &= -\frac{1}{g^2} \text{tr} \left( \bar{\psi}_\alpha (\Gamma^\mu)_{\alpha\beta} [A_\mu, \psi_\beta] \right), \end{aligned} \quad (2.1)$$

where  $A_\mu$  ( $\mu = 1, \dots, 4$ ) are traceless  $N \times N$  hermitean matrices, and  $\psi_\alpha, \bar{\psi}_\alpha$  ( $\alpha = 1, 2$ ) are traceless  $N \times N$  complex matrices. The measure is defined as

$$d\psi d\bar{\psi} = \prod_{\alpha=1}^2 \left[ \prod_{i,j=1}^N \left[ d(\psi_\alpha)_{ij} d(\bar{\psi}_\alpha)_{ij} \right] \delta \left( \sum_{i=1}^N (\psi_\alpha)_{ii} \right) \delta \left( \sum_{i=1}^N (\bar{\psi}_\alpha)_{ii} \right) \right], \quad (2.2)$$

$$dA = \prod_{\mu=1}^4 \left[ \prod_{i < j} \{d \text{Re}(A_\mu)_{ij} d \text{Im}(A_\mu)_{ij}\} \prod_{i=1}^N \{d(A_\mu)_{ii}\} \delta \left( \sum_{i=1}^N (A_\mu)_{ii} \right) \right]. \quad (2.3)$$

This model is invariant under 4D Lorentz transformations,<sup>3</sup> where  $A_\mu$  transforms as a vector and  $\psi_\alpha$  as a Weyl spinor.  $\Gamma_\mu$  are  $2 \times 2$  matrices acting on the spinor indices, and they can be given explicitly as

$$\Gamma_1 = i\sigma_1, \quad \Gamma_2 = i\sigma_2, \quad \Gamma_3 = i\sigma_3, \quad \Gamma_4 = \mathbf{1}. \quad (2.4)$$

The model is manifestly supersymmetric, and it also has a  $SU(N)$  symmetry

$$A_\mu \longrightarrow V A_\mu V^\dagger; \quad \psi_\alpha \longrightarrow V \psi_\alpha V^\dagger; \quad \bar{\psi}_\alpha \longrightarrow V \bar{\psi}_\alpha V^\dagger, \quad (2.5)$$

where  $V \in SU(N)$ . All these symmetries are inherited from the super Yang-Mills theory before dimensional reduction. The model can be regarded as the four-dimensional counterpart of the IIB matrix model [2].

In contrast to unitary matrix models, where the integration domain for the partition function is compact, the first non-trivial question to be addressed in hermitean matrix models in general, is whether the model is well defined as it stands. The problem can be most clearly understood by decomposing the hermitean matrices into eigenvalues and angular variables, where a potential danger of divergence exists in the integration over the eigenvalues, even at finite  $N$ . This issue has been addressed numerically for the supersymmetric case [14] at  $N = 3$  as well as the bosonic case [12] up to  $N = 6$ . Exact results are available for  $N = 2$  [28]. There is also a perturbative argument which is valid when all the eigenvalues are well separated from

---

<sup>3</sup>When one defines the IIB matrix model non-perturbatively, a Wick rotation to euclidean signature is needed. This is also the case for the present model. Hence by Lorentz invariance we actually mean rotational invariance.

each other [13, 19]. This reasoning agrees with the conclusions obtained for small  $N$  [12, 14, 28]. In particular, supersymmetric models in  $D = 4, 6, 10$  are expected to be well defined for arbitrary  $N$ . Our simulations confirm that this is indeed the case for  $D = 4$ .

Since the model is well defined without any cutoff, the parameter  $g$ , which is the only parameter of the model, can be absorbed by rescaling the variables,

$$A_\mu = g^{1/2} X_\mu, \quad (2.6)$$

$$\psi_\alpha = g^{3/4} \Psi_\alpha. \quad (2.7)$$

Therefore,  $g$  is a scale parameter rather than a coupling constant, i.e. the  $g$  dependence of physical quantities is completely determined on dimensional grounds. The parameter  $g$  should be tuned appropriately as one sends  $N$  to infinity, so that each correlation function of Wilson loops has a finite large- $N$  limit. Whether such a limit really exists or not is one of the dynamical issues we address in this work.

We now discuss the Eguchi-Kawai equivalence [7], which is the equivalence between reduced models and the corresponding gauge theories in the large- $N$  limit. In its proof based on the Schwinger-Dyson equation, one has to assume quantities of the type

$$\langle \text{tr}(e^{ik_\mu A_\mu}) \text{tr}(e^{-ik_\mu A_\mu}) \rangle \quad (k_\mu \neq 0) \quad (2.8)$$

to vanish. Assuming in addition large- $N$  factorization, the vanishing of (2.8) is equivalent to  $\langle \text{tr}(e^{ik_\mu A_\mu}) \rangle = 0$ , which is guaranteed if the eigenvalues of  $A_\mu$  are uniformly distributed on the whole real axis in the large- $N$  limit. The fact that the present model is well defined without any cutoff implies that the eigenvalue distribution of  $A_\mu$  is *not* uniform, but it has a finite extent for finite  $N$ . Hence, the Eguchi-Kawai equivalence is quite non-trivial even in the supersymmetric case. Here the situation is more subtle than in the case of the unitary matrix model version of a large- $N$  reduced model [7]. There, the model has the  $(\mathbb{Z}_N)^D$  symmetry  $U_\mu \rightarrow e^{2\pi im_\mu/N} U_\mu$  ( $m_\mu = 0, 1, \dots, N-1$ ), hence quantities like  $\langle \text{tr}(U_\mu)^n \rangle$  vanish, unless the symmetry is spontaneously broken.

One might be tempted to consider a model defined by the partition function (2.1) but without imposing the traceless condition on  $A_\mu$ . We denote such a model as the  $U(N)$  model, to be distinguished from the original model, which we call the  $SU(N)$  model. The  $U(N)$  model has the  $U(1)^4$  symmetry

$$A_\mu \longrightarrow A_\mu + \alpha_\mu \mathbf{1}_N, \quad (2.9)$$

where  $\alpha_\mu$  is a real vector. Note, however, that the trace part of  $A_\mu$  in the  $U(N)$  model simply decouples because  $A_\mu$  appears in the action only through commutators. The transformation (2.9) acts on the decoupled trace part and hence it cannot play any physical rôle. Indeed the quantity (2.8) calculated with the  $U(N)$  model or with the  $SU(N)$  model is exactly the same. Thus, considering the  $U(N)$  model does not help.

Next we comment on the method we use to study the model. Details can be found in appendix A. The integration over fermionic variables can be done explicitly and the result is given by  $\det \mathcal{M}$ ,  $\mathcal{M}$  being a  $2(N^2 - 1) \times 2(N^2 - 1)$  complex matrix which depends on  $A_\mu$ . Hence the system we want to simulate can be written in terms of bosonic variables as

$$Z = \int dA e^{-S_b} \det \mathcal{M}. \quad (2.10)$$

A crucial point for the present work is that the determinant  $\det \mathcal{M}$  is actually real positive, as we prove in appendix A. Due to this property, we can introduce a  $2(N^2 - 1) \times 2(N^2 - 1)$  hermitean positive matrix  $\mathcal{D} = \mathcal{M}^\dagger \mathcal{M}$ , so that  $\det \mathcal{M} = \sqrt{\det \mathcal{D}}$ , and the effective action of the system takes the form

$$S_{\text{eff}} = S_b - \frac{1}{2} \ln \det \mathcal{D}. \quad (2.11)$$

We apply the Hybrid R algorithm [18] to simulate this system. In the framework of this algorithm, each update of a configuration is made by solving a hamiltonian equation for a fixed “time”  $\tau$ . The algorithm is plagued by a systematic error due to the discretization of  $\tau$  that we used to solve the equation numerically. We performed simulations at three different values of the time step  $\Delta\tau$ . Except in figure 2, we find that the results do not depend much on  $\Delta\tau$  (below a certain threshold), so we just present the results for the value  $\Delta\tau = 0.002$ , which appears to be sufficiently small.

We also note that there is an exact result

$$\langle \text{tr } F^2 \rangle = - \left\langle \text{tr} \left( \sum_{\mu \neq \nu} [A_\mu, A_\nu]^2 \right) \right\rangle = 6g^2(N^2 - 1), \quad (2.12)$$

which can be obtained by a scaling argument, similar to the one used for the bosonic case [13]. We used this exact result to check the code and the numerical accuracy.

### 3. The space-time structure

We first study the space-time structure of the reduced model. In the IIB matrix model, the eigenvalues of the bosonic matrices  $A_\mu$  are interpreted as the space-time coordinates [2, 6, 19, 20]. However, since the matrices  $A_\mu$  are not simultaneously diagonalizable in general, the space-time is not classical. In order to extract the space-time structure, we first define the space-time uncertainty  $\Delta$  by

$$\Delta^2 = \frac{1}{N} \text{tr}(A_\mu^2) - \max_{U \in \text{SU}(N)} \frac{1}{N} \sum_i \{(UA_\mu U^\dagger)_{ii}\}^2, \quad (3.1)$$

which is invariant under Lorentz transformation and  $\text{SU}(N)$  transformation (2.5) [13]. This formula has been derived in ref. [13] based on analogy to quantum mechanics, regarding  $A_\mu$  as an operator acting on a space of states. It has the natural property

that  $\Delta^2$  vanishes if and only if the matrices  $A_\mu$  are diagonalizable simultaneously. For each configuration  $A_\mu$  generated by a Monte Carlo simulation, we maximize  $\sum_i \{(UA_\mu U^\dagger)_{ii}\}^2$  with respect to the  $SU(N)$  matrix  $U$ . We denote the matrix which yields the maximum as  $U_{\max}$ , and we define  $x_{\mu i} = (U_{\max} A_\mu U_{\max}^\dagger)_{ii}$  as the space-time coordinates of  $N$  points ( $i = 1, \dots, N$ ) in four-dimensional space-time.

Note that  $x_{\mu i}$  should be identified with the dynamical variables denoted by the same  $x_{\mu i}$  in ref. [19]. There, the bosonic matrices  $A_\mu$  and the fermionic matrices  $\psi_\alpha$  are decomposed into diagonal and off-diagonal elements as

$$\begin{aligned}(A_\mu)_{ij} &= x_{\mu i} \delta_{ij} + a_{\mu ij} \quad (a_{\mu ii} = 0), \\ (\psi_\alpha)_{ij} &= \xi_{\alpha i} \delta_{ij} + \varphi_{\alpha ij} \quad (\varphi_{\alpha ii} = 0).\end{aligned}\tag{3.2}$$

The off-diagonal parts  $a_{\mu ij}$  and  $\varphi_{\alpha ij}$  are integrated out using the “Lorentz gauge” in the one-loop approximation, which is valid when the points  $x_{\mu i}$  ( $i = 1, \dots, N$ ) are well separated from each other. Thus one obtains the effective action for  $x_{\mu i}$  and  $\xi_{\alpha i}$ , which can be considered as a low-energy effective action of the supersymmetric large- $N$  reduced model. In order to get the effective action only for  $x_{\mu i}$ , one still has to integrate over  $\xi_{\alpha i}$ , which cannot be done exactly for  $D = 6$  and  $D = 10$  (IIB matrix model). In  $D = 4$ , however, the integration over  $\xi_{\alpha i}$  can be carried out exactly and the system of  $x_{\mu i}$  is described by a simple branched polymer with an attractive potential between the points connected by a bond. In  $D = 6$  and  $D = 10$ , the system of  $x_{\mu i}$  is expected to be described by some complicated branched-polymer like structure. Thus, although the one-loop approximation might seem quite drastic, the low-energy effective theory of  $x_{\mu i}$  still has a non-trivial dynamics. In ref. [19], some plausible mechanisms for the collapse of the  $x_{\mu i}$  distribution in IIB matrix model have been discussed. What we have described in the previous paragraph provides a way to extract the low-energy effective theory of  $x_{\mu i}$  from the full model without perturbative expansions. In particular, we can check explicitly whether the one-loop approximation adopted in ref. [19] really captures the low-energy dynamics of the supersymmetric large- $N$  reduced model.

We first look at the distribution  $\rho(r)$  of the distances  $r$ , where the distance between two arbitrary points  $x_i \neq x_j$  is measured by  $\sqrt{(x_i - x_j)^2}$ . In figure 1 we plot the results for  $N = 16, 24, 32$  and  $48$ . We first note that the distribution at small  $r$  falls off rapidly below  $r/\sqrt{g} \sim 1.5$ , independently of  $N$ . (This behavior is also seen in the bosonic case shown in figure 10.) This observation is in agreement with the argument in ref. [19] that the ultraviolet behavior of the space-time structure of the model is controlled by the  $SU(2)$  matrix model. There, this argument has been used to justify the introduction of a  $N$ -independent ultraviolet cutoff in the low-energy effective theory, which otherwise suffers from ultraviolet divergence due to coinciding  $x_{\mu i}$ 's. Our observation confirms that the ultraviolet cutoff is indeed generated dynamically if one treats the full model non-perturbatively instead of making perturbative expansions around diagonal matrices.

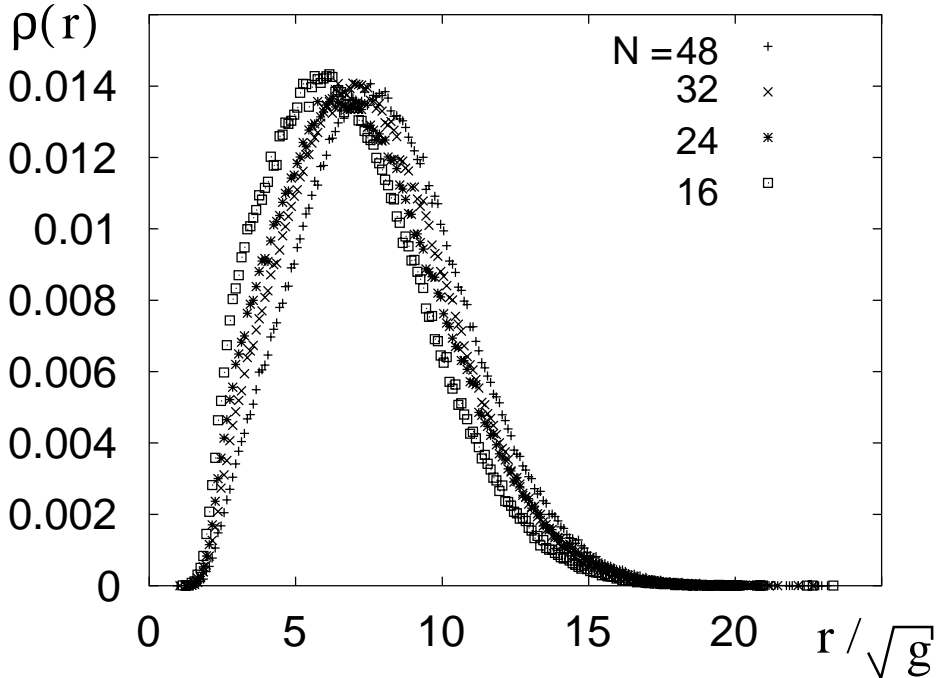


**Figure 1:** The distribution of distances  $\rho(r)$ , plotted against  $r/\sqrt{g}$  for  $N = 16, 24, 32$  and  $48$ .

In both, the supersymmetric as well as the bosonic case, we observe that the distribution shifts towards larger  $r$  as one increases  $N$ . In order to quantify this behavior, we define the extent of space-time by

$$R_{\text{new}} = \frac{2}{N(N-1)} \left\langle \sum_{i < j} \sqrt{(x_i - x_j)^2} \right\rangle = \int_0^\infty dr \, r \rho(r). \quad (3.3)$$

We denote this quantity by  $R_{\text{new}}$  in order to distinguish it from the definition of the extent of the space-time  $R = \sqrt{\langle \frac{1}{N} \text{tr}(A_\mu^2) \rangle}$  used in ref. [13].  $R$ , which roughly corresponds to  $\sqrt{\langle \int_0^\infty dr \, r^2 \rho(r) \rangle}$ , is logarithmically divergent in the 4D supersymmetric case due to the asymptotic behavior  $\rho(r) \sim r^{-3}$  at large  $r$  [15]. On the other hand,  $R_{\text{new}}$  does not suffer from this divergence as eq. (3.3) shows. In figure 2 we plot the results for the space-time extent  $R_{\text{new}}$  as well as those for the space-time uncertainty  $\sqrt{\langle \Delta^2 \rangle}$  for  $N = 16, 24, 32$  and  $48$ . We repeat the same measurements for the bosonic model with  $N$  up to  $256$  and include the results in figure 2 for comparison. We see that the effect of fermions enhances  $R_{\text{new}}$  and suppresses  $\sqrt{\langle \Delta^2 \rangle}$  considerably. However, the power of the large- $N$  behavior does not seem to be affected.

Let us discuss the results for  $R_{\text{new}}$ . In the bosonic case, the data can be nicely fitted to a power behavior with  $R_{\text{new}}/\sqrt{g} = 1.56(1) \cdot N^{1/4}$ . As expected, the observed large- $N$  behavior of  $R_{\text{new}}$  is the same as the one obtained for  $R$  in ref. [13]. In the supersymmetric case, the large- $N$  behavior of  $R_{\text{new}}$  can be predicted by the branched

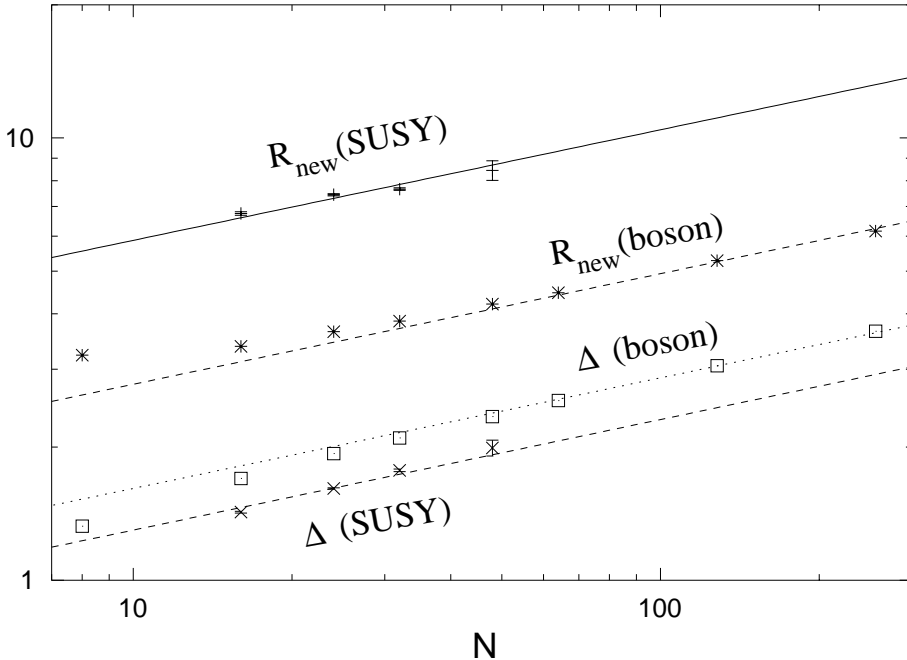


**Figure 2:**  $R_{\text{new}}/\sqrt{g}$  and  $\sqrt{\langle \Delta^2 \rangle/g}$ , plotted against  $N$ . The results for the bosonic model are also included. The lines are fits to the power behavior  $\propto N^{1/4}$ , which is predicted theoretically. (In the labels we use a short-hand notation.)

polymer picture based on the one-loop approximation [19]. Since the Hausdorff dimension of branched polymers is four,  $d_H = 4$ , the number of points  $N$  grows as the extent  $R_{\text{new}}$  of the branched polymer,  $N \sim (R_{\text{new}}/\ell)^{d_H}$ . Here  $\ell$  is the minimum length of the bond, which is of  $O(\sqrt{g})$  as we have already discussed. Thus one obtains  $R_{\text{new}} \sim \sqrt{g} N^{1/4}$ . The data in figure 2 seem to be consistent with this prediction. Fitting the data to this power behavior, we obtain  $R_{\text{new}}/\sqrt{g} = 3.30(1) \cdot N^{1/4}$ .

One might be surprised that supersymmetry does not affect the power of the large- $N$  behavior of the space-time extent  $R_{\text{new}}$ . We recall, however, that in the bosonic case the explanation is completely different — although the power is the same [13]. There the one-loop perturbative expansion around diagonal matrices yields a logarithmic attractive potential between all the pairs of eigenvalues. The one-loop effective potential is dominant as far as the extent of the eigenvalue distribution is larger than  $\sqrt{g} N^{1/4}$ . One can therefore put an upper bound on the space-time extent  $R \lesssim \sqrt{g} N^{1/4}$ . What happens actually is that this upper bound is saturated. The behavior  $R \sim \sqrt{g} N^{1/4}$  can also be shown to all orders in the  $1/D$  expansion [13].

Let us turn to the results for the space-time uncertainty. Using the one-loop perturbative expansion,  $\langle \Delta^2 \rangle$  can be roughly estimated as

$$\langle \Delta^2 \rangle = \frac{1}{N} \sum_{ij} \langle a_{\mu ij} a_{\mu ji} \rangle = \frac{1}{N} \sum_{ij} \left\langle \frac{g^2}{(x_i - x_j)^2} \right\rangle \sim \frac{g^2 N}{R_{\text{new}}^2}. \quad (3.4)$$

The powers of  $R_{\text{new}}$  and  $\sqrt{\langle \Delta^2 \rangle}$ , as well as the coefficients we observe, are in

qualitative agreement with this estimation. The bosonic case has been studied before in ref. [13]. The data in figure 2 can be nicely fitted to a power behavior with  $\sqrt{\langle \Delta^2 \rangle/g} = 0.907(3) \cdot N^{1/4}$ . Thus, in the bosonic case we obtain  $\sqrt{\langle \Delta^2 \rangle} \sim 0.58 R_{\text{new}}$  [13], which indicates a significant deviation from the classical space-time picture. On the other hand, in the supersymmetric case we obtain  $\sqrt{\langle \Delta^2 \rangle/g} = 0.730(2) \cdot N^{1/4}$ , hence our result amounts to  $\sqrt{\langle \Delta^2 \rangle} \sim 0.22 R_{\text{new}}$ , coming closer to the classical space-time picture.

We will see in the next section that the scale parameter  $g$  should be taken to be  $O(1/\sqrt{N})$  in order to obtain a universal scaling behavior for the Wilson loop correlators. This means that the space-time uncertainty in the physical scale remains finite, rather than vanishing, in the large- $N$  limit. Therefore the present model satisfies the space-time uncertainty principle proposed for non-perturbative definitions of string theories [21].

#### 4. Wilson loop correlation functions

In the interpretation of a large- $N$  reduced model as a string theory, Wilson loop operators correspond to string creation operators [8]. Therefore, the existence of a non-trivial large- $N$  limit of the Wilson loop correlators is an absolutely crucial issue. It has been addressed before in the 2D Eguchi-Kawai model, where non-trivial large- $N$  scaling has indeed been observed [10].

We define the “Wilson loop” and the “Polyakov line” operators as

$$W(k) = \frac{1}{N} \text{tr} (e^{ikX_1} e^{ikX_2} e^{-ikX_1} e^{-ikX_2}), \quad P(k) = \frac{1}{N} \text{tr} (e^{ikX_1}), \quad (4.1)$$

where  $X_\mu$  are dimensionless matrices defined in eq. (2.6). For convenience we have chosen particular components of  $X_\mu$  in the above definitions, but the choice of the directions becomes irrelevant when taking the vacuum expectation value, due to Lorentz symmetry and parity invariance. In the actual calculations we take an average over all possible choices of the components in order to enhance the statistics.

The real parameter  $k$  represents the dimensionless “momentum” that characterizes the momentum density distributed along the string. The physical (dimensionful) momentum variable is given by  $k_{\text{phys}} = k/\sqrt{g}$ . We have to tune  $g$  depending on  $N$ , so that the correlation functions of the above operators have definite large- $N$  limits as functions of  $k_{\text{phys}}$ . In the following, we always set  $g = 1$  for  $N = 48$  without loss of generality.

In all plots except for figure 4, we further assume  $g$  to be proportional to  $1/\sqrt{N}$ . This turns out to be consistent with large- $N$  scaling, hence  $g \propto 1/\sqrt{N}$  can be regarded as one of our observations.

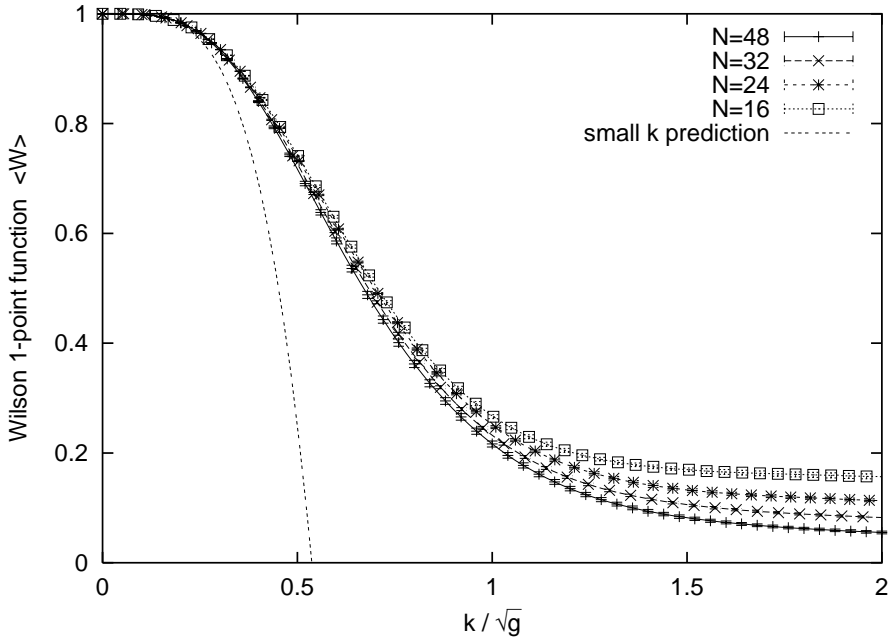


**Figure 3:** The Wilson 1-point function  $\langle W \rangle$ , plotted against  $k_{\text{phys}} = k/\sqrt{g}$ .

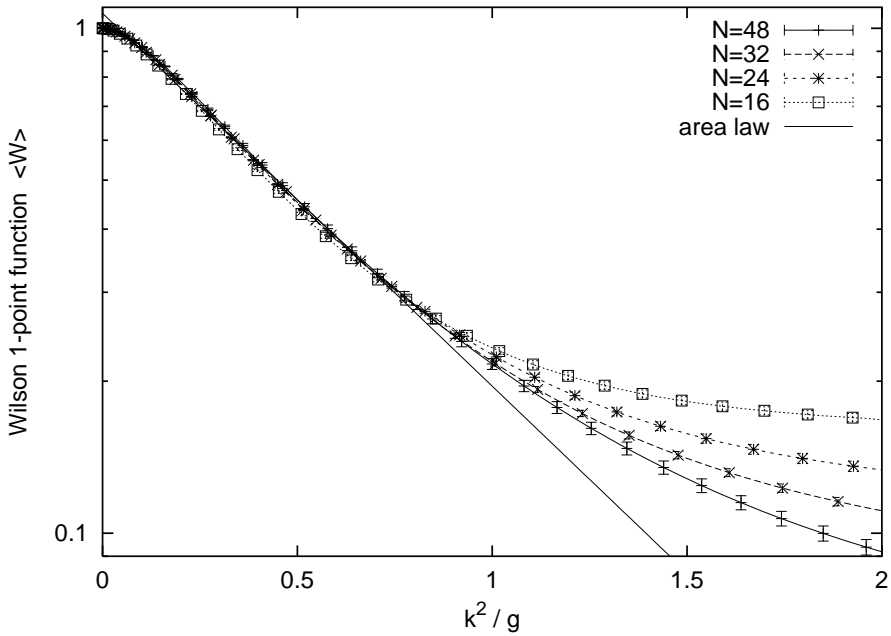


**Figure 4:** The Wilson 1-point function  $\langle W \rangle$  is plotted now logarithmically against  $k^2/g$ , in order to visualize the extent of the area law behavior. The scale parameter  $g$  has been tuned as described in the text.

#### 4.1 One-point function and Eguchi-Kawai equivalence

In this subsection we discuss the one-point functions, and we start with the Wilson loop  $\langle W(k) \rangle$ . Also ref. [16] presents some recent results about this quantity.

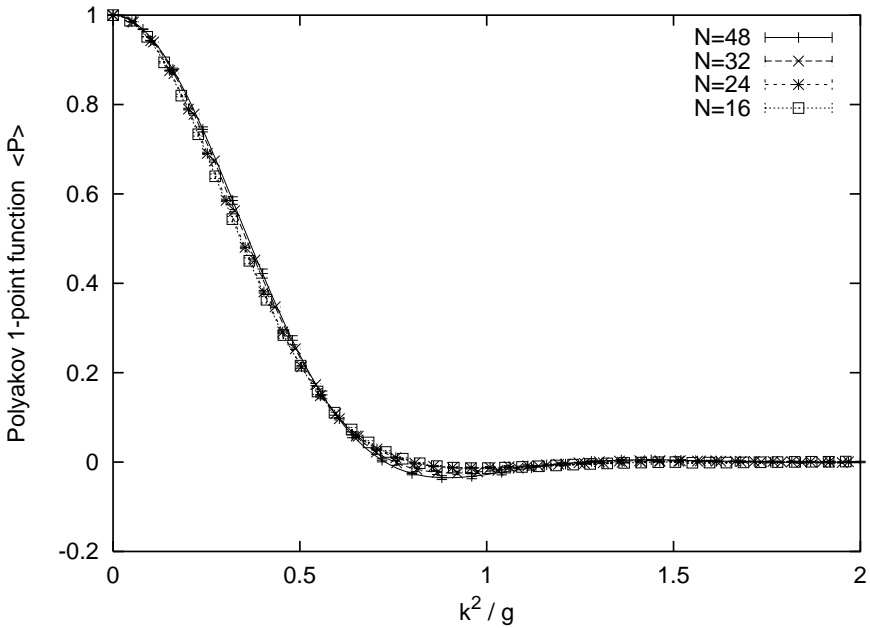


**Figure 5:** The Polyakov 1-point function  $\langle P \rangle$ , plotted against  $k/\sqrt{g}$ .

In the small  $k$  regime it can be expanded as

$$\langle W(k) \rangle = 1 + \frac{1}{2N} k^4 \langle \text{tr}([X_1, X_2]^2) \rangle + O(k^6) = 1 - \frac{1}{4} k^4 \left( N - \frac{1}{N} \right) + O(k^6), \quad (4.2)$$

where we have used the exact result (2.12). Therefore, in order to make the small  $k$  regime scale, we have to take  $g \propto 1/\sqrt{N}$ , as we mentioned above. In figure 3 we plot  $\langle W(k) \rangle$  against  $k/\sqrt{g}$ . The small  $k$  region scales as it should, and the results agree with the analytical prediction (4.2). Moreover the scaling extends up to  $k/\sqrt{g} = O(1)$ .

If the model is equivalent to ordinary gauge theory — namely to 4D pure super Yang-Mills theory with four supercharges — which is confining, then the Wilson loop should exhibit an area law behavior. In order to illustrate this behavior, we show a logarithmic plot of  $\langle W(k) \rangle$  versus the area  $k^2/g$  in figure 4. In this figure only, we fine-tune  $g$  as a function of  $N$  so that the scaling in the intermediate regime of  $k$  becomes even better. We stay with the convention  $g(48) = 1$  and use the optimal values  $g(32) = 1.291$ ,  $g(24) = 1.563$ ,  $g(16) = 1.929$ , which is not far from  $g \propto 1/\sqrt{N}$ . The small deviation can be understood as a manifestation of finite- $N$  effects. Figure 4 shows indeed a region of  $k$  that corresponds to the area law behavior  $\langle W(k) \rangle \sim \exp(-\text{const.}k^2)$ . Surprisingly, the area law behavior is also observed in the bosonic model, as figure 12 shows, which is quite contrary to what one might have expected [13, 16]. In both cases, supersymmetric and bosonic, it is not clear from the data whether the area law extends to  $k = \infty$  in the large- $N$  limit. We will discuss the observed area law behavior from a theoretical point of view later.

We now proceed to the one-point function of the Polyakov line. In the 2D Eguchi-Kawai model [10] this quantity vanishes due to  $(\mathbb{Z}_N)^D$  symmetry. In the present model, however, there is no exact symmetry that could make such a quantity vanish, as we explained in section 2. Note for instance that  $P(k = 0) = 1$  for any configuration. Figure 5 shows the results for  $\langle P(k) \rangle$ . It falls off rapidly as  $k$  increases.<sup>4</sup> Again we observe a good scaling with  $g \propto 1/\sqrt{N}$ . Remember also that  $\langle P(k) \rangle$  is actually just a Fourier transform of the eigenvalue distribution. Therefore, the value of  $k$  at which  $\langle P(k) \rangle$  drops to zero, which we denote as  $k_0$ , should be inversely proportional to the space-time extent  $R_{\text{new}}$ . The observed scaling with  $g \propto 1/\sqrt{N}$  is consistent with our result in the previous section,  $R_{\text{new}} \sim \sqrt{g} N^{1/4}$ . The result for the bosonic case is shown in figure 13. We obtain a similar behavior except for some oscillations in the large- $k$  region. In particular, scaling is confirmed with  $g \propto 1/\sqrt{N}$ . The value of  $k_0$  is larger than the supersymmetric  $k_0$ , as expected. The ratio of  $k_0$  in the two cases is indeed roughly the inverse of the corresponding ratio of  $R_{\text{new}}$  (the bosonic  $k_0$  is about twice as large as the supersymmetric one).

The above observations concerning  $\langle P(k) \rangle$  and  $R_{\text{new}}$  have an interesting implication on the Eguchi-Kawai equivalence. We recall that from the results for  $\langle W(k) \rangle$ , we phenomenologically concluded that the Eguchi-Kawai equivalence holds at least in a finite range of scale for both, the supersymmetric and the bosonic case. We would like to understand this from a theoretical point of view. As we mentioned in section 2, in the proof of Eguchi-Kawai equivalence,  $\langle P(k) \rangle$  is assumed to vanish. We have found that  $\langle P(k) \rangle$  is indeed small for  $k > k_0$ , but not for  $k < k_0$ . This means that the proof works for  $k > k_0$ , but not for small  $k$ , which corresponds to the ultraviolet regime in the corresponding gauge theory. We also observed that  $k_0$  remains finite with respect to a physical scale in the large- $N$  limit. A complementary understanding can be obtained by taking Gross-Kitazawa's point of view [24]. As explained in ref. [13], the extent of the eigenvalue distribution of  $A_\mu$  determines the momentum cutoff of the corresponding gauge theory [24]. The observation in section 3 that  $R_{\text{new}} \sim \sqrt{g} N^{1/4}$  implies that the momentum cutoff remains finite in physical scale as  $N \rightarrow \infty$ . Let us assume that the momentum cutoff is finite, but large enough to attract the renormalization flow to the fixed point which corresponds to the universality class of gauge theory. Then the flow follows closely the renormalization trajectory of the gauge theory, in a certain regime. That would explain why the equivalence holds at least in a finite range of scale. However, since the momentum cutoff does not go to infinity in the large- $N$  limit, it is conceivable that the renormalization flow will leave the renormalization trajectory of the gauge theory at some low-energy scale eventually. In this case the observed area law would not extend to  $k = \infty$  even in the large- $N$  limit.

---

<sup>4</sup>One may consider the small  $k$  expansion here, as in eq. (4.2). The result is  $\langle P(k) \rangle = 1 - \frac{1}{2N} k^2 \langle \text{tr}(X_1^2) \rangle + \dots$ . The fact that  $\langle \text{tr}(A_\mu^2) \rangle$  is logarithmically divergent means that actually  $\langle P(k) \rangle$  has a non-analytic behavior  $\sim 1 + \text{const. } k^2 \ln |k|$  around  $k = 0$ .

## 4.2 Multi-point functions and universal scaling

In this subsection we proceed to the large- $N$  scaling of multi-point functions of Wilson loops. We first note that in the bosonic case, there are analytical results to all order in the  $1/D$  expansion [13]. The statement is that

$$\langle \mathcal{O}_1 \mathcal{O}_2 \cdots \mathcal{O}_n \rangle_{\text{con}} \sim O\left(\frac{1}{N^{2(n-1)}}\right) \quad \text{for the bosonic case,} \quad (4.3)$$

where  $\mathcal{O}_i$  denotes a Wilson loop or a Polyakov line as defined in eq. (4.1), and  $\langle \cdots \rangle_{\text{con}}$  means that only the connected part is taken. The correlation functions should be considered as functions of  $k_{\text{phys}} = k/\sqrt{g}$ , where  $g$  is taken to be proportional to  $1/\sqrt{N}$ . Our results for the bosonic model shown in figures 11 to 17 clearly confirm this analytical prediction. Let us consider a wave-function renormalization for each operator,  $\mathcal{O}_i^{(\text{ren})} = Z \mathcal{O}_i$ , so that connected correlation functions of the renormalized operators  $\mathcal{O}_i^{(\text{ren})}$  become finite in the large- $N$  limit. Relation (4.3) means, however, that we cannot make all the multi-point functions finite. If we make the two-point functions finite by choosing  $Z \sim O(N)$ , then all the higher-point functions vanish in the large- $N$  limit. In the supersymmetric case, we will see that scaling is observed again with  $g \propto 1/\sqrt{N}$ , but in contrast to the bosonic case a universal  $Z$  that makes all the correlators finite seems to exist. In the following, we always set  $Z(N=48)=1$ , without loss of generality.

Let us start with the two-point functions, for which we measure the following two correlation functions,

$$G_2^{(W)}(k) = \langle \{\text{Im } W(k)\}^2 \rangle, \quad G_2^{(P)}(k) = \langle \{\text{Im } P(k)\}^2 \rangle. \quad (4.4)$$

We take the imaginary part in order to avoid subtraction of a disconnected part.<sup>5</sup> (Note in this regard that since  $\text{Im } W(k)$  and  $\text{Im } P(k)$  are parity odd, the one-point functions  $\langle \text{Im } W(k) \rangle$  and  $\langle \text{Im } P(k) \rangle$  vanish due to parity invariance of the model.) The results are shown in figures 6 and 7, respectively. If we multiply the data by  $(N/48)^2$ , they scale nicely with  $g \propto 1/\sqrt{N}$ .

As a three-point function, we measure

$$G_3^{(W)}(k) = \langle (\text{Im } W(k))^2 \text{Re } W(k) \rangle - \langle (\text{Im } W(k))^2 \rangle \langle \text{Re } W(k) \rangle. \quad (4.5)$$

We multiply the data either by  $(N/48)^3$ , which is required for the universal scaling of all the multi-point correlation functions, or by  $(N/48)^4$ , which is the factor predicted for the bosonic model. The results are compared in figure 8. We do observe a nice scaling behavior with a factor of  $(N/48)^3$ , but the scaling becomes worse for a factor of  $(N/48)^4$ .

---

<sup>5</sup>We also measured a number of multi-point functions, which are not presented here since the relative errors are rather large.

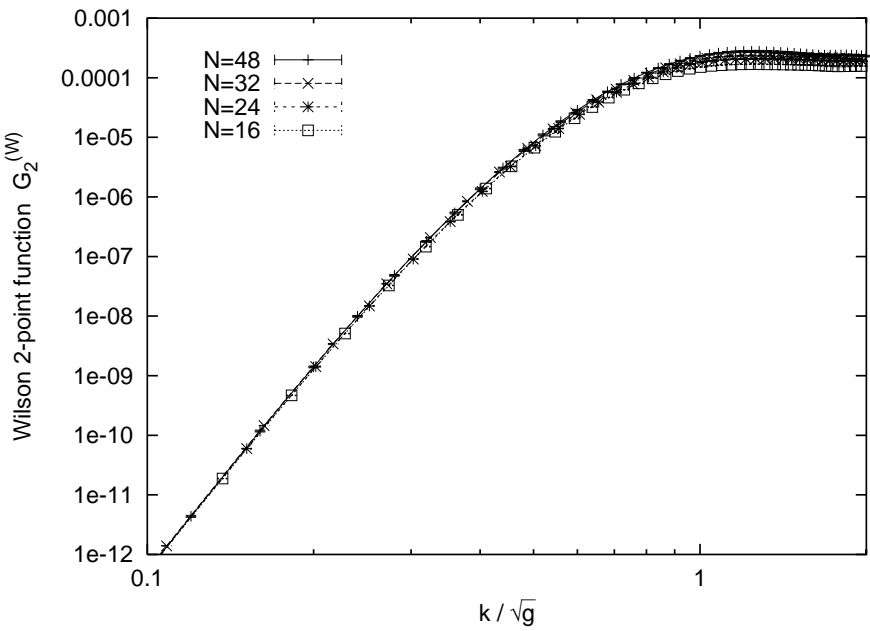


**Figure 6:** The Wilson 2-point function  $G_2^{(W)}$ , multiplied by  $Z^2 \propto N^2$ , plotted against  $k/\sqrt{g}$ .

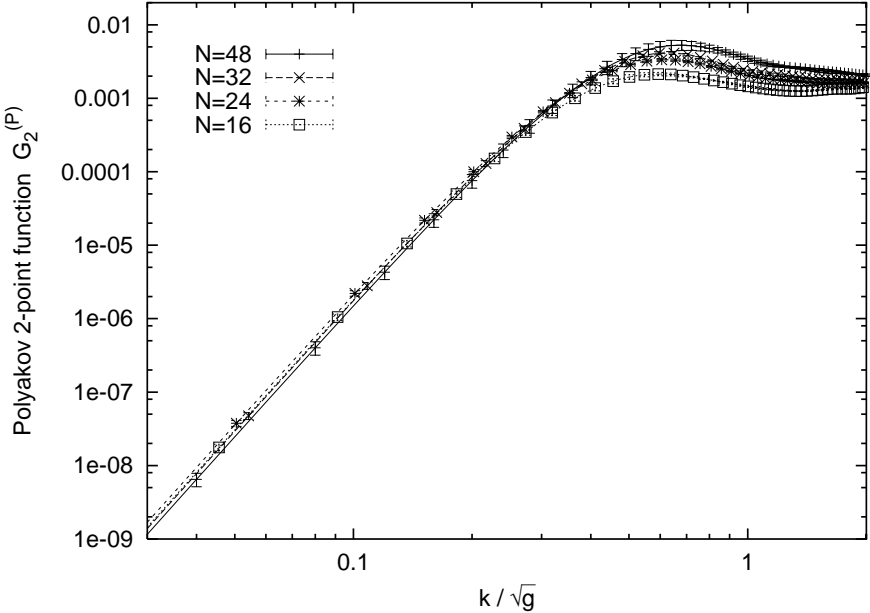


**Figure 7:** The Polyakov 2-point function  $G_2^{(P)}$ , multiplied by  $Z^2 \propto N^2$ , plotted against  $k/\sqrt{g}$ .

Similarly, as a four-point function we measure

$$G_4^{(W)}(k) = \langle (\text{Im } W(k))^4 \rangle - 3\langle (\text{Im } W(k))^2 \rangle. \quad (4.6)$$

We multiply the data either by  $(N/48)^4$ , which is required for the universal scaling of

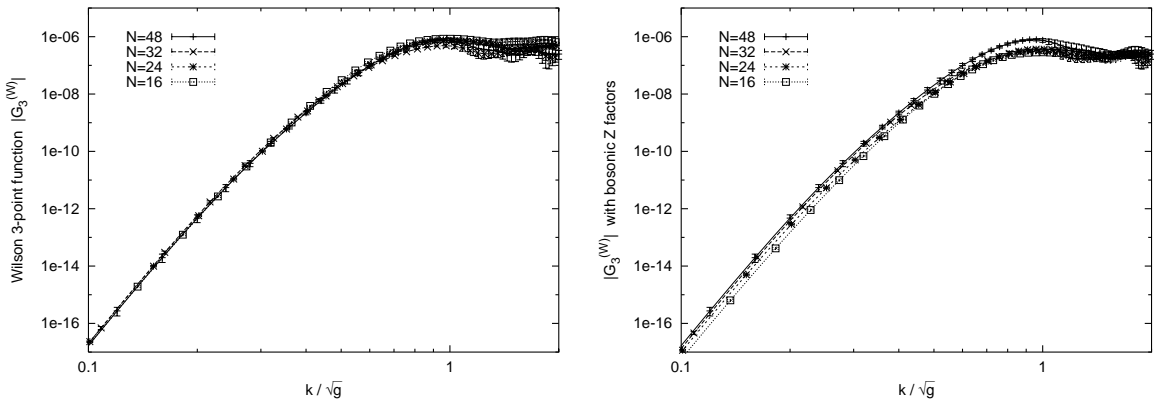


**Figure 8:** The Wilson 3-point function  $G_3^{(W)}$ , multiplied by  $Z^3 \propto N^3$ , plotted against  $k/\sqrt{g}$  on the left. On the right we show the corresponding plot using the bosonic prediction  $Z^3 \propto N^4$  instead, which leads to an inferior level of scaling.

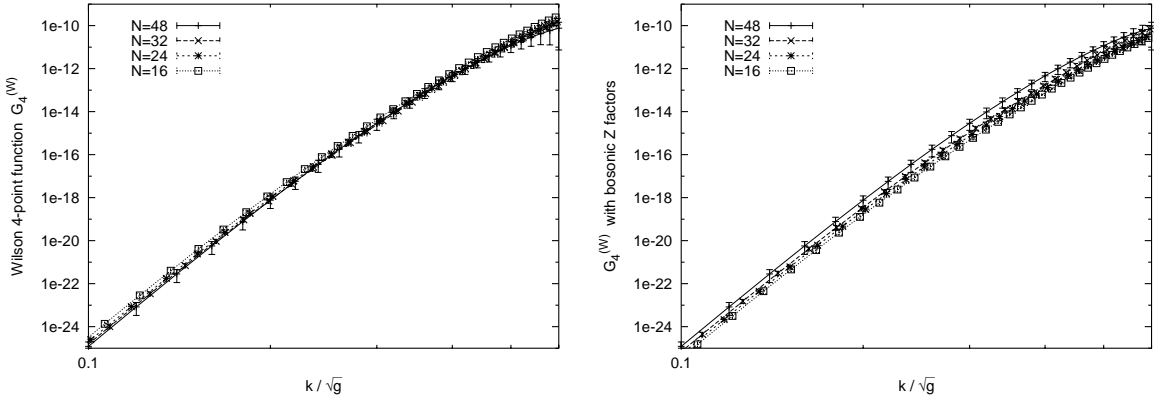


**Figure 9:** The Wilson 4-point function  $G_4^{(W)}$ , multiplied by  $Z^4 \propto N^4$ , plotted against  $k/\sqrt{g}$  on the left. On the right we show the corresponding plot using the bosonic prediction  $Z^4 \propto N^6$  instead, which leads to an inferior level of scaling.

all the multi-point correlation functions, or by  $(N/48)^6$ , which is the factor predicted for the bosonic model. The results are compared in figure 9. Again the scaling behavior obtained with the factor for universal scaling is superior over the behavior with the bosonic factor.

To summarize our results concerning Wilson loop correlators, we observe that

$$\langle \mathcal{O} \rangle \sim O(1), \quad \langle \mathcal{O}_1 \mathcal{O}_2 \cdots \mathcal{O}_n \rangle_{\text{con}} \sim O\left(\frac{1}{N^n}\right) \quad \text{for } n \geq 2. \quad (4.7)$$

These correlators scale as functions of  $k_{\text{phys}} = k/\sqrt{g}$ , where  $g$  is taken to be proportional to  $1/\sqrt{N}$ . This means that all the multi-point functions of the renormalized operators  $\mathcal{O}_i^{(\text{ren})} = Z \mathcal{O}_i$  become finite in the large- $N$  limit if we set  $Z \sim O(N)$ , in contrast to the bosonic case. We will discuss further the implications of this universal scaling behavior in the next subsection.

Finally we comment on large the  $N$  factorization. In ordinary gauge theory, large- $N$  factorization can be shown by weak-coupling expansion as well as strong-coupling expansion. In a large- $N$  reduced model with hermitean matrices, one cannot do a weak-coupling or a strong-coupling expansion, because  $g$  is not a coupling constant but a scale parameter, as we have mentioned. Hence large- $N$  factorization is non-trivial. In the bosonic case, large- $N$  factorization holds to all orders of the  $1/D$  expansion [13]. Our observation (4.7) implies

$$\langle \mathcal{O}_1 \mathcal{O}_2 \cdots \mathcal{O}_n \rangle = \langle \mathcal{O}_1 \rangle \langle \mathcal{O}_2 \rangle \cdots \langle \mathcal{O}_n \rangle + O\left(\frac{1}{N^2}\right), \quad (4.8)$$

where the  $O(1/N^2)$  contributions are due to  $\langle \mathcal{O}_1 \mathcal{O}_2 \rangle_{\text{con}} \langle \mathcal{O}_3 \rangle \cdots \langle \mathcal{O}_n \rangle$ , etc. Therefore the large- $N$  factorization is also valid in the supersymmetric case.

### 4.3 Interpretation of the large- $N$ scaling

In this subsection, we discuss the physical meaning of the large- $N$  scaling (4.7) we observed.

If one views large- $N$  reduced models as a non-perturbative definition of string theory by identifying Wilson loops as creation and annihilation operators of fundamental strings, string unitarity requires a large- $N$  behavior of the form  $N^{a\chi_n}$  for the connected correlators of  $n$  Wilson loops, where  $\chi_n = 2 - n$  is the Euler characteristic of the worldsheet. In order to compare this behavior to our results for the supersymmetric case (4.7) as well as for the bosonic case (4.3), we first drop the extra factor  $1/N^n$  in (4.3) and (4.7), which is due to the normalization (4.1) of the operators  $\mathcal{O}_i$ . Then we find that the connected correlators of Wilson loops change from an  $O(N^{\chi_n})$  behavior to an  $O(1)$  behavior by the introduction of supersymmetry. Our results for the supersymmetric case indicate  $a = 0$ , which implies that one is far away from the perturbative regime in genus. From the string theoretical point of view this indicates that the supersymmetric large- $N$  reduced model might automatically realize a kind of “double-scaling limit” [29], which played a crucial rôle in a non-perturbative formulation of non-critical bosonic string theory using matrix models. While we do not presently have an analytic understanding of the observed large- $N$  behavior for the supersymmetric case, we give a possible diagrammatic explanation and discuss how the double-scaling limit can be realized. Our argument also suggests that smooth worldsheet configurations dominate in the diagrammatic representation of the multi-point correlation functions in the supersymmetric case, but not in the bosonic case.

We estimate  $n$ -point correlation functions of Wilson loops using the perturbative expansion (3.2), along the lines of refs. [19, 13]. Again we drop the factor  $1/N$  in the operators  $\mathcal{O}_i$  in (4.1). Let us start with the bosonic case. By integrating out the off-diagonal elements perturbatively, we obtain Feynman diagrams, where the diagonal

elements  $x_i$  are assigned to every index loop. Each diagram can be evaluated using the Feynman rules and the result can be written schematically as

$$\mathcal{F} = \sum_{i_1, \dots, i_F} \left( \frac{g^2}{(x_i - x_j)^2} \right)^L \left( (x_k - x_l) \frac{1}{g^2} \right)^{V_3} \left( \frac{1}{g^2} \right)^{V_4}, \quad (4.9)$$

where  $F$ ,  $L$ ,  $V_3$ ,  $V_4$  are the number of index loops (faces), propagators (links), 3-point and 4-point vertices, respectively. They obey the relations

$$F + V - L = \chi, \quad 4V_4 + 3V_3 = 2L, \quad V = V_3 + V_4. \quad (4.10)$$

Here  $\chi$  is the Euler characteristic of the diagram given as  $\chi = 2 - 2h - n$ , where  $h$  is the genus (the number of handles in the diagram) and  $n$  is the number of the Wilson loops, which form the boundaries of the diagram. Next we have to take an ensemble average of (4.9) over the distributions  $\{x_i\}$  obtained from the configurations. Given a configuration in the ensemble, quantities such as  $(x_i - x_j)$  in (4.9) are generically of the order of the extent of the  $x_i$ -distribution, which is given by  $R \sim \sqrt{g} N^{1/4}$  as we discussed in section 3. Considering such contributions only, we can estimate the sum (4.9) as

$$\mathcal{F} \sim N^F \left( \frac{g^2}{R^2} \right)^L \left( \frac{R}{g^2} \right)^{V_3} \left( \frac{1}{g^2} \right)^{V_4} \sim N^\chi. \quad (4.11)$$

Thus we can reproduce the large- $N$  behavior of the correlation functions for the bosonic model. If we view the diagrams as worldsheets and the  $x_i$ 's as embedding coordinates of the worldsheet into the target space, the above contributions correspond to a *rough* worldsheet. Points on the worldsheet which are connected by a link (as  $x_i$  and  $x_j$  in (4.9)) are embedded in the target space quite randomly.<sup>6</sup>

In the supersymmetric case, the fermion diagonal elements make the perturbative estimation of the correlation functions much more complicated. However, let us naively consider the expression (4.9) and take an ensemble average over the distributions of  $x_i$ . Since the extent of the  $x_i$ -distribution has the same large- $N$  power behavior as in the bosonic case, the estimate given in the previous paragraph is valid also in the supersymmetric case. This explains the observed behavior of the one-point and two-point functions, but for the three-point functions, the estimate is  $O(N)$  smaller than the observed large- $N$  behavior. As possible contributions that might explain this observation, let us consider the case when the  $x_i$ 's, which are connected in a given diagram, are as close to each other as the actual distribution of  $x_i$ 's allows. Such contributions correspond to the case when the worldsheet is *smooth*. In fact we have seen in figure 1 that there seems to be a *minimal length*  $\ell$ , which is of the order  $\sqrt{g}$ , characterizing the distribution of  $|x_i - x_j|$ . Replacing  $|x_i - x_j|$  with

---

<sup>6</sup>The dominance of rough worldsheet configurations in the bosonic case was also suggested in ref. [13] based on the saturation of the upper bound for  $R$  obtained by perturbation theory.

this minimal length, the summand of (4.9) becomes

$$\left(\frac{g^2}{\ell^2}\right)^L \left(\frac{\ell}{g^2}\right)^{V_3} \left(\frac{1}{g^2}\right)^{V_4} \sim O(1). \quad (4.12)$$

Let us denote by  $n_N$  the number of such terms appearing in the sum over the indices  $i_1, \dots, i_F$  in (4.9). Then we can estimate this kind of contribution to (4.9) as

$$\mathcal{F} \sim \langle n_N \rangle \cdot O(1), \quad (4.13)$$

where  $\langle n_N \rangle$  is the average of  $n_N$  over the configurations of  $x_i$ . In the bosonic case, the result (4.3) requires  $\langle n_N \rangle$  to be smaller than any negative power of  $N$ . Namely the probability that a term such as (4.12) appears in the sum (4.9) should decrease rapidly as  $N$  increases. In the supersymmetric case, on the other hand, the observed large- $N$  behavior of the three-point functions can be explained by the contributions (4.13) assuming that  $\langle n_N \rangle$  is of  $O(1)$ . Note also that for the one-point and two-point functions, the contributions (4.13) with  $\langle n_N \rangle \sim O(1)$  is at most the same order as the contributions (4.11), so that the agreement obtained by considering only (4.11) is not affected by taking account of the additional contributions of (4.13). For the  $\langle n_N \rangle$  to be of  $O(1)$ , there should be a finite probability that an arbitrary number of  $x_i$ 's come close to forming a “network” with the link length of order  $O(\ell)$ . Whether this really occurs or not is itself an interesting dynamical question, which can be addressed directly by examining the configurations of  $x_i$  obtained as in section 3. We leave this issue for future investigations.

If the above argument is correct, it implies that in the supersymmetric case,  $n$ -point functions for  $n \geq 3$  are dominated by contributions which correspond to *smooth* worldsheets.<sup>7</sup> Furthermore, it implies that they are independent of the genus  $h$ , and consequently that diagrams of all topologies contribute in the large- $N$  limit. This is reminiscent of the double-scaling limit in matrix models [29], which we review briefly for comparison.

Let us consider a hermitean one-matrix model with the partition function

$$Z = \int d\phi e^{-S}; \quad S = N (\text{tr } \phi^2 - \lambda \text{tr } \phi^3), \quad (4.14)$$

$\phi$  being a  $N \times N$  hermitean matrix. Although the model as it stands is ill-defined for finite  $N$  due to the unbounded action  $S$ , the perturbative vacuum  $\phi = 0$  becomes stable in the large- $N$  limit when the coupling constant  $\lambda$  is below a critical value  $\lambda_c$ . The  $n$ -point correlation function of operators  $\text{tr } \phi^{l_i}$  ( $i = 1, \dots, n$ ) can be defined as

$$f_n(l_1, \dots, l_n; \lambda, N) = \langle \text{tr } \phi^{l_1} \cdots \text{tr } \phi^{l_n} \rangle, \quad (4.15)$$

---

<sup>7</sup>This is reminiscent of the fact that an increased smoothness of the bosonic part in a supersymmetric worldsheet has been observed in toy models for superstrings [30].

where  $l_i$  are integers. A perturbative expansion of this quantity with respect to the coupling constant  $\lambda$  gives Feynman diagrams, each of which corresponds to a triangulation of two-dimensional manifold with  $n$  boundaries of length  $l_i$ . Thus the matrix model can be interpreted as a model of non-critical bosonic strings regarding the two-dimensional manifold as a worldsheet of the strings. Since the power of  $\lambda$  for each diagram is given by the number of triangles in the triangulated surface, the coupling constant  $\lambda$  can be interpreted as an exponential of the bare cosmological constant of the worldsheet. Introducing a “lattice spacing”  $\epsilon$  as the link length of the triangulated surface, the physical (dimensionful) quantities corresponding to the length of the boundaries and the cosmological constant can be introduced as

$$\tilde{l}_i = \epsilon l_i(\epsilon), \quad t = \frac{1}{\epsilon^2} \ln \frac{\lambda_c}{\lambda(\epsilon)}, \quad (4.16)$$

where  $\lambda_c$  is the critical coupling constant defined below (4.14). A continuum limit  $\epsilon \rightarrow 0$  should be taken in such a way that these quantities are fixed.

The contributions to (4.15) from all the diagrams which have  $h$  handles are known to behave asymptotically for  $\epsilon \rightarrow 0$  as (see, for example, ref. [31])

$$f_n \left( \frac{\tilde{l}_1}{\epsilon}, \dots, \frac{\tilde{l}_n}{\epsilon}; \lambda_c e^{-t\epsilon^2}, N \right) \sim (N\epsilon^{5/2})^{2-2h-n} \epsilon^{-n}. \quad (4.17)$$

From this expression, one can see that there are two ways to take the large- $N$  limit. The planar limit corresponds to taking the large- $N$  limit first at fixed  $\epsilon$ , followed by the continuum limit  $\epsilon \rightarrow 0$ . In this limit, only the planar diagrams, which have  $h = 0$  handles, survive and the  $n$ -point correlation functions behave as  $O(N^{2-n})$ . The double-scaling limit, on the other hand, corresponds to taking the large- $N$  limit and the continuum limit  $\epsilon \rightarrow 0$  simultaneously, fixing  $N\epsilon^{5/2} = g_{\text{str}}^{-1} t^{-5/4}$ . The dimensionless parameter  $g_{\text{str}}$  can be interpreted as the string coupling constant since the  $n$ -point correlation function becomes proportional to  $(g_{\text{str}})^{-\chi}$ , where  $\chi$  is again the Euler characteristic of the diagram. Thus, all the diagrams with different  $h$  survive in this limit. Furthermore, by absorbing the remaining power behavior  $\epsilon^{-n}$  into the renormalization of each operator, we find that the  $n$ -point correlation function behaves as  $O(1)$ , which means that all the multi-point correlation functions become finite. Note that string perturbation theory corresponds to a perturbative expansion with respect to the string coupling constant  $g_{\text{str}}$ . In the double-scaling limit of the matrix model,  $g_{\text{str}}$  appears as a tunable parameter, which does not have to be small. Therefore, the double-scaling limit of the matrix model can be regarded as a non-perturbative formulation of non-critical bosonic string theory.

The scaling behaviors observed in the large- $N$  reduced model for the bosonic and supersymmetric case formally coincide with the scaling behaviors found in the planar limit and the double-scaling limit of the matrix model, respectively. We note, however, that in the large- $N$  reduced model, we do not have the parameter

corresponding to  $\lambda$ . In this sense, one might say that the double-scaling limit is taken automatically in the supersymmetric large- $N$  reduced model, and that the string coupling constant  $g_{\text{str}}$  is not a tunable parameter but is fixed *dynamically*. We recall that within perturbative string theory, the string coupling constant  $g_{\text{str}}$ , which is related to the vacuum expectation value of the dilaton field, is a moduli parameter and cannot be fixed dynamically. Our argument suggests the interesting possibility that the vacuum expectation value of the dilaton field is no longer a moduli parameter and is fixed dynamically if superstring theory is treated *non-perturbatively*.<sup>8</sup> It is also intriguing that the qualitative difference of the large- $N$  behavior from the bosonic case might be related to the dominance of smooth worldsheet configurations.

## 5. Summary and discussion

In this paper, we have studied the large- $N$  dynamics of a supersymmetric large- $N$  reduced model by means of Monte Carlo simulations.

We studied the space-time structure represented by the eigenvalues of the bosonic matrices. In particular, we found that the large- $N$  power behavior of the space-time extent is consistent with the branched-polymer picture based on the one-loop perturbative expansion around diagonal matrices. The effect of fermions in the space-time extent was observed by the enhancement of the coefficient in the power behavior, but not in the power itself. The power appears to be the same for the bosonic and supersymmetric case. We emphasized, however, that the theoretical explanation is completely different. We also found that the space-time uncertainty is clearly reduced for the supersymmetric case, which means that space-time comes closer to the classical behavior. Even in the supersymmetric case, the space-time uncertainty is found to be finite in the physical scale in the large- $N$  limit. We argued that this implies that the model satisfies the uncertainty principle for the non-perturbative definition of superstring theory.

The large- $N$  scaling behavior of Wilson loop correlators is observed at fixed  $g^2 N$ . Although this scaling of  $g$  is the same as in the bosonic model, there is a striking difference from the bosonic case in the wave-function renormalization with the multi-point functions. In the bosonic case, there was no universal scaling behavior: keeping two-point functions finite, all the higher-point functions vanish. In the supersymmetric case, we observed a clear trend for all the higher-point functions to become finite in the large- $N$  limit. We gave a perturbative argument that this result for the supersymmetric case might be understood if we assume smooth worldsheets to dominate. This argument also implies that all the topologies of the worldsheet contribute with equal weight to the amplitude. All these features are reminiscent of the double scaling limit of matrix models.

---

<sup>8</sup>Such a possibility has also been discussed in ref. [19].

We also addressed the issue of Eguchi-Kawai equivalence. By searching for the area law behavior in the one-point function of the Wilson loop, we concluded that the equivalence does hold at least in a finite region of scale. What is rather surprising is that the area law behavior has been observed also for the bosonic model. This suggests that the bosonic model is also equivalent to ordinary large- $N$  Yang-Mills theory at least in a finite region of scale, which is contrary to what has been generally believed. We argued, however, that this conclusion can be understood from a more theoretical point of view based on the large- $N$  behavior obtained for  $R_{\text{new}}$  and the one-point function of the Polyakov line. It is an open question whether this equivalence extends to the far infrared regime.

To summarize, we have gained new insight into the dynamical properties of the large- $N$  behavior of a supersymmetric large- $N$  reduced model. We hope that our findings shed light on the dynamical aspects of the most interesting 10D version of our model, i.e. the IIB matrix model. In this respect, it is encouraging that the large- $N$  scaling of Wilson loop correlators in the present model has been observed at fixed  $g^2 N$ , which coincides with the result obtained by requiring that the loop equations of the IIB matrix model should reproduce the string field hamiltonian. We presume that a large- $N$  scaling of Wilson loop correlators — like the one we observed — also holds for the IIB matrix model; then the only difference would be the spontaneous breakdown of Lorentz symmetry. One of the good news revealed in the present work is that low-energy effective theory, based on the one-loop approximation, does already capture the low-energy dynamics of the supersymmetric matrix model. We therefore hope to address the most interesting issue of spontaneous breakdown of Lorentz invariance by using the low-energy effective theory — which is in 10D far more complicated than in the 4D case. We are going to report on Monte Carlo studies of IIB matrix model along these lines in the near future.

## Acknowledgments

We are grateful to T. Ishikawa, C.F. Kristjansen, Y.M. Makeenko, T. Nakajima, M. Staudacher, A. Tsuchiya and G. Vernizzi for valuable discussions. J.A. thanks MaPhySto, the Centre for Mathematical Physics and Stochastics, funded by a grant from The Danish National Research Foundation, as well as ESF, the European Science Foundation, for financial support. K.N.A. acknowledges partial support from a postdoctoral fellowship from the Greek Institute of National Fellowships (IKY). J.N. is supported by the Japan Society for the Promotion of Science as a Postdoctoral Fellow for Research Abroad. The computation has been done partly on Fujitsu VPP500 at High Energy Accelerator Research Organization (KEK), Fujitsu VPP700E at The Institute of Physical and Chemical Research (RIKEN), and NEC SX4 at Research Center for Nuclear Physics (RCNP) of Osaka University. This work is supported by the Supercomputer Project (No.99-53) of KEK.

## A. The algorithm for the Monte Carlo simulation

In this appendix, we explain the algorithm we use for the Monte Carlo simulation of the supersymmetric matrix model. Only in this appendix we set  $g = 1$  for simplicity.

We first carry out the integration over fermionic matrices to obtain the explicit formula for the fermion determinant. We calculate

$$Z_f[A] = \int d\psi d\bar{\psi} e^{-S_f}, \quad (\text{A.1})$$

where we use the notation introduced in eq. (2.1). We define a set of generators  $t^a \in \text{gl}(N, \mathbb{C})$  by

$$(t^a)_{ij} = \delta_{ii_a} \delta_{jj_a} \quad (a = 1, \dots, N^2), \quad (\text{A.2})$$

where  $i_a$  and  $j_a$  are integers running from 1 to  $N$ , specified uniquely by

$$a = N(i_a - 1) + j_a. \quad (\text{A.3})$$

We also introduce the notation  $\bar{a} = N(j_a - 1) + i_a$ . The fermionic matrix  $\psi_\alpha$  can be expanded in terms of  $t^a$  as

$$(\psi_\alpha)_{ij} = \sum_{a=1}^{N^2} \psi_{a\alpha} (t^a)_{ij}, \quad (\text{A.4})$$

where  $\psi_{a\alpha} = (\psi_\alpha)_{ia_ja}$ .  $\bar{\psi}_\alpha$  and  $A_\mu$  can be expanded similarly with the coefficients  $\bar{\psi}_{a\alpha} = (\bar{\psi}_\alpha)_{i_a j_a}$  and  $A_{a\mu} = (A_\mu)_{i_a j_a}$ . Note also that  $A_{\bar{a}\mu} = (A_{a\mu})^*$  due to the Hermiticity of  $A_\mu$ .

We define the structure constants  $g_{abc}$  of  $\text{gl}(N, \mathbb{C})$  by

$$g_{abc} = \text{tr}(t^c [t^a, t^b]) = \delta_{ja_ib} \delta_{jb_ic} \delta_{jc_ia} - \delta_{jc_ib} \delta_{jb_ia} \delta_{ja_ic}. \quad (\text{A.5})$$

The fermionic action then reads

$$S_f = -g_{abc} \bar{\psi}_{c\alpha} (\Gamma_\mu)_{\alpha\beta} A_{a\mu} \psi_{b\beta} = -\bar{\psi}_{a\alpha} \mathcal{M}'_{a\alpha, b\beta} \psi_{b\beta}, \quad (\text{A.6})$$

where

$$\mathcal{M}'_{a\alpha, b\beta} = -g_{abc} (\Gamma_\mu)_{\alpha\beta} A_{c\mu}. \quad (\text{A.7})$$

We first integrate out  $(\psi_\alpha)_{NN}$  and  $(\bar{\psi}_\alpha)_{NN}$  using the  $\delta$  functions in the measure (2.2). We get a factor of  $1/N^4$  followed by the replacements

$$(\psi_\alpha)_{NN} \implies - \sum_{j=1}^{N-1} (\psi_\alpha)_{jj}; \quad (\bar{\psi}_\alpha)_{NN} \implies - \sum_{j=1}^{N-1} (\bar{\psi}_\alpha)_{jj} \quad (\text{A.8})$$

in the fermionic action. The integration over the remaining Grassmann variables

yields  $\det \mathcal{M}$ , where  $\mathcal{M}$  is the  $2(N^2 - 1) \times 2(N^2 - 1)$  complex matrix defined by

$$\mathcal{M}_{a\alpha,b\beta} = \mathcal{M}'_{a\alpha,b\beta} - \mathcal{M}'_{N^2\alpha,b\beta}\delta_{i_a j_a} - \mathcal{M}'_{a\alpha,N^2\beta}\delta_{i_b j_b} \quad (\text{A.9})$$

(the indices  $a$  and  $b$  run from 1 to  $N^2 - 1$ ). Thus, we obtain

$$Z_f[A] = \frac{1}{N^4} \det \mathcal{M}. \quad (\text{A.10})$$

We first want to show that the determinant  $\det \mathcal{M}$  is real positive.<sup>9</sup> For this purpose we note that the matrix  $\mathcal{M}$  satisfies the identity  $\sigma_2 \mathcal{M} \sigma_2 = \mathcal{M}^*$ . Hence if  $\varphi_{a\alpha}$  is an eigenvector of  $\mathcal{M}$  with an eigenvalue  $\lambda$ , then  $\psi_{a\alpha} = (\sigma_2)_{\alpha\beta}(\varphi_{a\beta})^*$  is an eigenvector of  $\mathcal{M}$  with an eigenvalue  $\lambda^*$ . It is important that the two vectors  $\varphi_{a\alpha}, \psi_{a\alpha}$  are linearly independent. The determinant, which is the product of all the eigenvalues of  $\mathcal{M}$ , should therefore be real and positive semi-definite. In the case of 6D or 10D (IIB matrix model) versions of the supersymmetric large- $N$  reduced model, the fermion integral yields a complex effective action in general. This causes the notorious sign problem, which makes standard Monte Carlo simulations practically inapplicable for large  $N$ . In the present case, since the determinant  $\det \mathcal{M}$  is real positive, we can introduce a  $2(N^2 - 1) \times 2(N^2 - 1)$  hermitean matrix  $\mathcal{D} = \mathcal{M}^\dagger \mathcal{M}$ , which has real positive eigenvalues, and  $\det \mathcal{M} = \sqrt{\det \mathcal{D}}$ . Therefore we have written the effective action for the bosonic matrices  $A_\mu$  in eq. (2.11) as

$$S_{\text{eff}} = S_b - \frac{1}{2} \ln \det \mathcal{D}. \quad (\text{A.11})$$

We apply the Hybrid R algorithm [18] to simulate this system.<sup>10</sup>

The first step of the Hybrid R algorithm is to apply the molecular dynamics method [34]. We introduce a conjugate momentum for  $A_{a\mu}$  as  $X_{a\mu}$ , which satisfies  $X_{\bar{a}\mu} = (X_{a\mu})^*$ . The partition function can be re-written as

$$Z = \int dX dA e^{-H}, \quad (\text{A.12})$$

where  $H$  is the ‘‘hamiltonian’’ defined by

$$H = \frac{1}{2} \sum_{\mu a} X_{\bar{a}\mu} X_{a\mu} + S_b[A] - \frac{1}{2} \ln \det \mathcal{D}. \quad (\text{A.13})$$

The update of  $X_{a\mu}$  can be done by just generating  $X_{a\mu}$  with the probability distribution  $\exp(-\frac{1}{2} \sum |X_{a\mu}|^2)$ . In order to update  $A_{a\mu}$ , we use the hamiltonian equations

$$\frac{dA_{a\mu}(\tau)}{d\tau} = \frac{\partial H}{\partial X_{a\mu}} = X_{\bar{a}\mu}, \quad (\text{A.14})$$

$$\frac{dX_{a\mu}(\tau)}{d\tau} = -\frac{\partial H}{\partial A_{a\mu}} = \frac{1}{2} \text{tr} \left( \frac{\partial \mathcal{D}}{\partial A_{a\mu}} \mathcal{D}^{-1} \right) - \frac{\partial S_b}{\partial A_{a\mu}}. \quad (\text{A.15})$$

---

<sup>9</sup>This has been already reported in ref. [14] as a numerical observation. For related work, see ref. [32].

<sup>10</sup>Ref. [33] gives an overview of effective algorithms for dynamical fermions, including the Hybrid R algorithm.

Along the “classical trajectory” given by the hamiltonian equation,

- (i)  $H$  is invariant,
- (ii) the motion is reversible,
- (iii) the phase-volume is preserved,

$$\frac{\partial(A(\tau), X(\tau))}{\partial(A(0), X(0))} = 1, \quad (\text{A.16})$$

where  $(A(\tau), X(\tau))$  is a point on the trajectory after evolution from  $(A(0), X(0))$ .

Therefore, generating a new set of  $(A, X)$  by solving the hamiltonian equation for a fixed “time” interval  $\tau$  satisfies detailed balance. This procedure — together with the proceeding generation of  $X_{a\mu}$  with the gaussian distribution — is called “one trajectory”, which corresponds to “one sweep” in ordinary Monte Carlo simulations.

In order to solve the hamiltonian equation numerically, we have to discretize the “time”  $\tau$ . A discretization which maintains the properties (ii) and (iii) is known. The slight violation of (i) for finite  $\Delta\tau$  causes systematic errors. One can in principle eliminate the systematic error completely, by making a Metropolis accept/reject decision at the end of each trajectory. But in the present case, the overhead for this procedure is rather large. We therefore decided to omit that step, and just use a sufficiently small  $\Delta\tau$ . Still we can use the specific discretization of ref. [18], which we explain below, to minimize the systematic error. As we explain later, we do find a good convergence in small  $\Delta\tau$ , and the systematic error is well under control.

We introduce a short-hand notation for the discretized  $X_{a\mu}(\tau)$  and  $A_{a\mu}(\tau)$ ,

$$X_{a\mu}^{(r)} = X_{a\mu}(r\Delta\tau); \quad A_{a\mu}^{(s)} = A_{a\mu}(s\Delta\tau). \quad (\text{A.17})$$

The hamiltonian equations are discretized as

$$\begin{aligned} A_{a\mu}^{(1/4)} &= A_{a\mu}^{(0)} + \frac{\Delta\tau}{4} X_{\bar{a}\mu}^{(0)}, & A_{a\mu}^{(n+1/2)} &= A_{a\mu}^{(n+1/4)} + \frac{\Delta\tau}{4} X_{\bar{a}\mu}^{(n)}, \\ A_{a\mu}^{(m+1/4)} &= A_{a\mu}^{(m-1/2)} + \frac{3\Delta\tau}{4} X_{\bar{a}\mu}^{(m)}, & A_{a\mu}^{(\nu)} &= A_{a\mu}^{(\nu-1/2)} + \frac{\Delta\tau}{2} X_{\bar{a}\mu}^{(\nu)}, \\ X_{a\mu}^{(n+1)} &= X_{a\mu}^{(n)} + \Delta\tau \left\{ \frac{1}{2} R_{a\mu}^{(n+1/2)} - \frac{\partial S_b}{\partial A_{a\mu}} (A_{a\mu}^{(n+1/2)}) \right\}, \end{aligned} \quad (\text{A.18})$$

where  $n = 0, 1, \dots, \nu - 1$ ,  $m = 1, \dots, \nu - 1$ , and  $R_{a\mu}^{(n+1/2)}$  is defined by

$$R_{c\mu}^{(n+1/2)} = \Phi_{a\alpha}^* \left( \frac{\partial \mathcal{D} (A_{a\mu}^{(n+1/2)})}{\partial A_{c\mu}} \right)_{a\alpha b\beta} \Phi_{b\beta}, \quad (\text{A.19})$$

$$\mathcal{D} (A_{a\mu}^{(n+1/2)}) \Phi = \mathcal{M}^\dagger (A_{a\mu}^{(n+1/4)}) \eta. \quad (\text{A.20})$$

Here  $\eta_{a\alpha}$  are complex variables generated by the gaussian distribution  $\exp(-\sum_{a\alpha} |\eta_{a\alpha}|^2)$ . The judicious choice of the argument of  $\mathcal{M}^\dagger$  is the tool to reduce the systematic error [18].

We solve eq. (A.20) with respect to  $\Phi$  by means of the conjugate gradient method [35], which is iterative. Each iteration involves a multiplication of the matrix  $\mathcal{D}$  with some vector  $v$ . Since  $\mathcal{D}$  is a  $2(N^2 - 1) \times 2(N^2 - 1)$  matrix, storing  $\mathcal{D}$  requires  $O(N^4)$  memory, and multiplying  $\mathcal{D}$  with  $v$  naively involves  $O(N^4)$  arithmetic operations. Actually we can do much better than this. We first recall that  $\mathcal{D} = \mathcal{M}^\dagger \mathcal{M}$ , where  $\mathcal{M}$  is the  $2(N^2 - 1) \times 2(N^2 - 1)$  matrix defined in eq. (A.9). The point is that the number of non-zero elements of  $\mathcal{M}$  is only  $O(N^3)$  (not  $O(N^4)$ ). Indeed, the multiplication  $\mathcal{M}v$  can be done economically as follows.

We consider

$$w_{a\alpha} = \mathcal{M}_{a\alpha b\beta} v_{b\beta}, \quad (\text{A.21})$$

and define the quantities  $w'_{a\alpha}$  and  $v'_{a\alpha}$ , where  $a$  runs from 1 to  $N^2$  as in  $\mathcal{M}'$ , by

$$v'_{a\alpha} = v_{a\alpha} \quad \text{for } a = 1, \dots, N^2 - 1, \quad v'_{N^2\alpha} = - \sum_{i_a=j_a} v_{a\alpha}, \quad (\text{A.22})$$

$$w'_{a\alpha} = \mathcal{M}'_{a\alpha b\beta} v'_{b\beta}. \quad (\text{A.23})$$

Now  $w_{a\alpha}$  can be written as

$$w_{a\alpha} = \begin{cases} w'_{a\alpha} - w'_{N^2\alpha} & \text{for } i_a = j_a \\ w'_{a\alpha} & \text{otherwise.} \end{cases} \quad (\text{A.24})$$

Thus the problem reduces to calculating the matrix-vector product in eq. (A.23). Using definition (A.7), we obtain

$$(w'_{\alpha})_{ij} = (\Gamma^\mu)_{\alpha\beta} [A_\mu, v'_\beta]_{ji}, \quad (\text{A.25})$$

where  $w'_\alpha$  and  $v'_\alpha$  are  $N \times N$  matrices associated with  $w'_{a\alpha}$  and  $v'_{a\alpha}$ , respectively, as in eq. (A.4). The commutator in eq. (A.25) requires  $O(N^3)$  arithmetic operations. Thus we save  $O(N)$  operations. In addition, we do not have to store neither  $g_{abc}$  nor  $\mathcal{M}$ . Multiplication of  $\mathcal{M}^\dagger$  with some vector  $v$  is done in the same way.

A similar technique should be used to calculate  $R_{a\mu}$  in eq. (A.19). Note first that it can be written as  $R_{c\mu} = T_{c\mu} + (T_{\bar{c}\mu})^*$ , where  $T_{c\mu}$  is given by

$$\begin{aligned} T_{c\mu} &= \Psi_{a\alpha} \left( \frac{\partial \mathcal{M}}{\partial A_{c\mu}} \right)_{a\alpha b\beta} \Phi_{b\beta}, \\ \Psi_{a\alpha} &= (\mathcal{M}_{a\alpha b\beta} \Phi_{b\beta})^*. \end{aligned} \quad (\text{A.26})$$

We define  $\Phi'$  and  $\Psi'$  in terms of  $\Phi$  and  $\Psi$ , as we defined  $v'$  in terms of  $v$  before in eq. (A.22). Now we can re-write  $T_{c\mu}$  as

$$T_{c\mu} = \frac{\partial}{\partial A_{c\mu}} \left( \Psi'_{a\alpha} (\mathcal{M}')_{a\alpha b\beta} \Phi'_{b\beta} \right). \quad (\text{A.27})$$

Using again eq. (A.7), we obtain

$$(T_\mu)_{ij} = -(\Gamma_\mu)_{\alpha\beta}[\Psi'_\alpha, \Phi'_\beta]_{ji}, \quad (\text{A.28})$$

where  $\Phi'_\alpha$ ,  $\Psi'_\alpha$  and  $T'_\mu$  are  $N \times N$  matrices associated with  $\Phi'_{a\alpha}$ ,  $\Psi'_{a\alpha}$  and  $T'_{a\mu}$ , respectively, as in eq. (A.4).

There are two parameters  $\nu$  and  $\Delta\tau$  in this algorithm. We can choose  $\nu\Delta\tau$  so that a typical autocorrelation time is minimized. We have taken  $\nu\Delta\tau = 1$  throughout the present work, and  $\nu = 200, 280, 500$  for each of the cases  $N = 16, 24, 32$ , and  $\nu = 500, 600$  for  $N = 48$ . Except in figure 2, we observed that the results are reasonably well converged at  $\nu = 500, \Delta\tau = 0.002$ , so we just present those results. For figure 2 we carried out an extrapolation to  $\Delta\tau = 0$  by assuming the  $\Delta\tau$  dependence of some observables  $Q(\Delta\tau)$  to be

$$Q(\Delta\tau) - Q(\Delta\tau = 0) \sim (\Delta\tau)^2 \cdot \langle \text{tr}(A_\mu^2) \rangle_{\Delta\tau}. \quad (\text{A.29})$$

This assumption has been checked for  $\langle \text{tr} F^2 \rangle$  with the exact result (2.12). We also observed that  $\langle \text{tr}(A_\mu^2) \rangle_{\Delta\tau}$  behaves as

$$\langle \text{tr}(A_\mu^2) \rangle_{\Delta\tau} \sim c_1 - c_2 \log \Delta\tau, \quad (\text{A.30})$$

for small  $\Delta\tau$ , where  $c_1$  and  $c_2$  are constants depending on  $N$ .<sup>11</sup> This implies that it diverges logarithmically for  $\Delta\tau \rightarrow 0$ , which is consistent with the theoretical prediction discussed below eq. (3.3).

Let us comment on the required computational effort of our algorithm. The dominant part comes from solving the linear system (A.20) using the conjugate gradient method. First of all, we find that the number of iterations necessary for the convergence of the method seems to grow linearly with the size of the matrix  $\mathcal{D}$ , namely as  $O(N^2)$ . This is much worse than the full QCD case with a fixed quark mass, where the number of iterations does not depend on the system size. We may interpret this phenomenon as a sort of “critical slowing down”, since the present system corresponds to QCD in the chiral limit. As we have seen, the number of arithmetic operations for each iteration is of order  $N^3$ . Therefore, the required computational effort of our algorithm is estimated to be  $O(N^5)$ .

For the bosonic case, we use the heat bath algorithm in the way proposed in ref. [13], which requires an effort of  $O(N^4)$ . We note, however, that application of a Hybrid Monte Carlo algorithm [36] allows for an  $O(N^3)$  algorithm for the bosonic case, which might be useful for proceeding to much larger  $N$ .

Finally, we give the numbers of configurations used for the measurements. For the supersymmetric case, they are 3060, 1508, 1296, 436 for  $N = 16, 24, 32, 48$ , respectively. For the bosonic case, we used 1000 configurations for each  $N$ .

---

<sup>11</sup>In QCD the  $\Delta\tau$  dependence of the systematic error is  $O(\Delta\tau^2)$  [18]. A similar argument leads to the assumption (A.29). Due to eq. (A.30), the  $\Delta\tau$  dependence of the systematic error in our case is expected to be  $(\Delta\tau)^2 \log \Delta\tau$ .

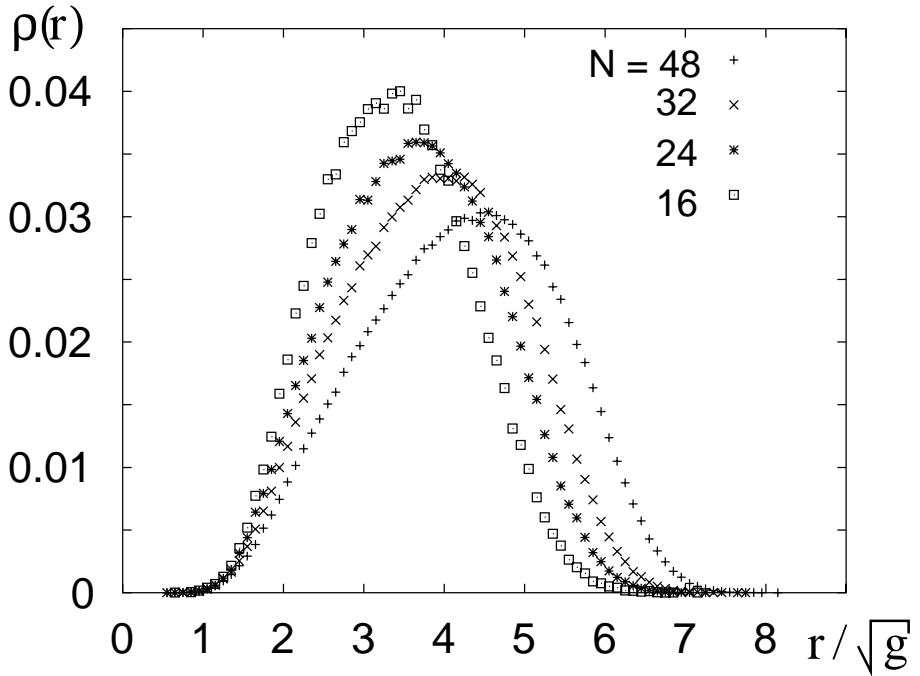


**Figure 10:** The bosonic distribution of distances  $\rho(r)$ , plotted against  $r/\sqrt{g}$  for  $N = 16$ ,  $24$ ,  $32$  and  $48$ .

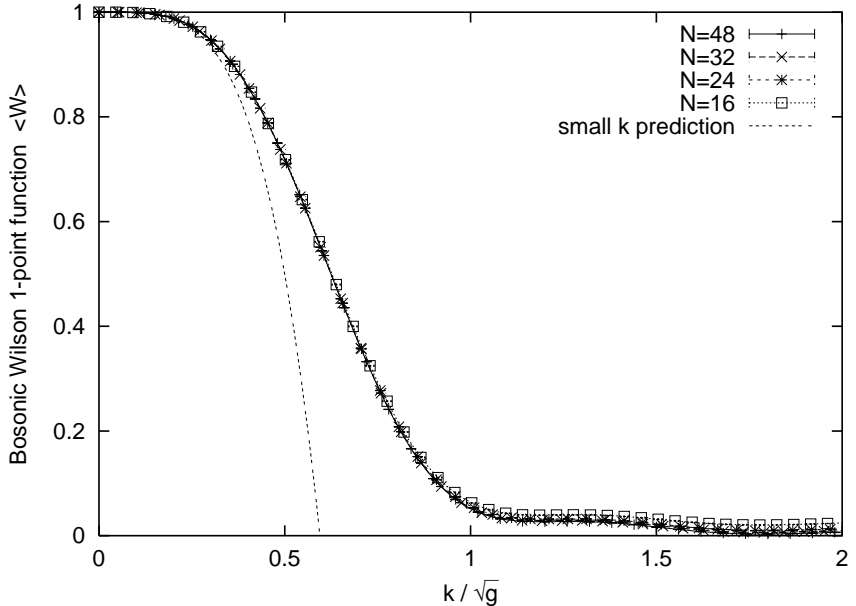


**Figure 11:** The bosonic Wilson 1-point function  $\langle W \rangle$ , plotted against  $k/\sqrt{g}$ . In this case, the small  $k$  prediction amounts to  $1 - (N/6)k^4$ .

## B. Results for the bosonic case

For comparison we show in this appendix the results for the bosonic case. By the bosonic case we mean a model obtained by just dropping the fermions from the

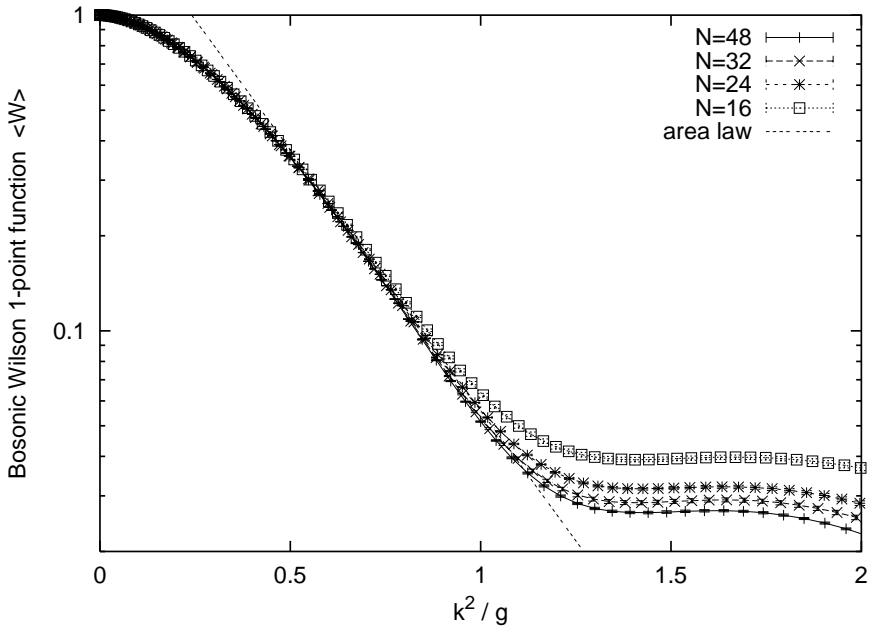


**Figure 12:** The bosonic Wilson 1-point function  $\langle W \rangle$  is plotted now logarithmically against  $k^2/g$ , in order to visualize the extent of the area law behavior.

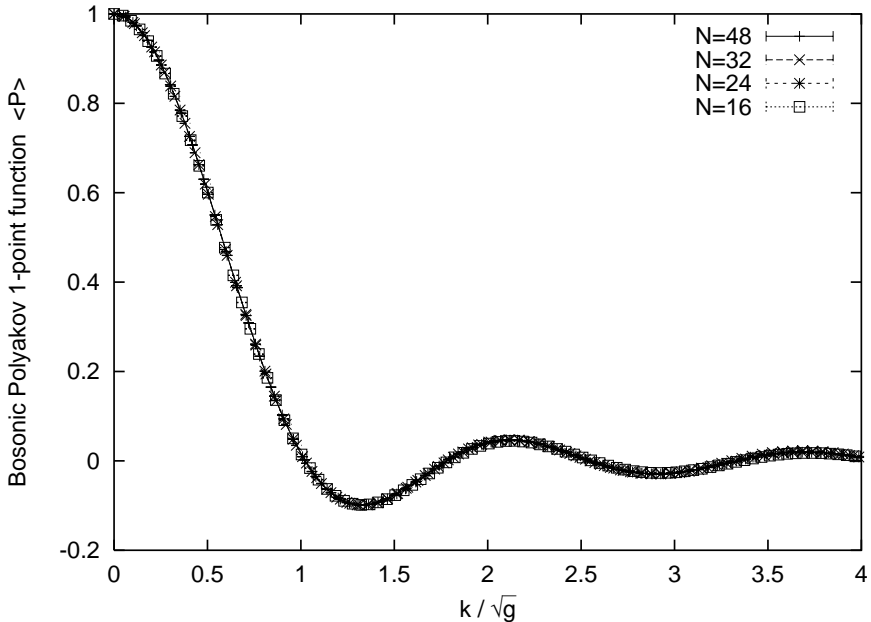


**Figure 13:** The bosonic Polyakov 1-point function  $\langle P \rangle$ , plotted against  $k/\sqrt{g}$ .

supersymmetric matrix model described by the partition function (2.1). Figure 10 shows the distribution  $\rho(r)$  defined in section 3. Figures 11 to 17 show the Wilson loop and Polyakov line correlators defined in section 4. We take  $g \propto 1/\sqrt{N}$  ( $g = 1$  for  $N = 48$ ) and plot the results against  $k_{\text{phys}} = k/\sqrt{g}$ , as in the supersymmetric case. We multiply the results by  $(N/48)^{2(n-1)}$  for  $n$ -point functions.

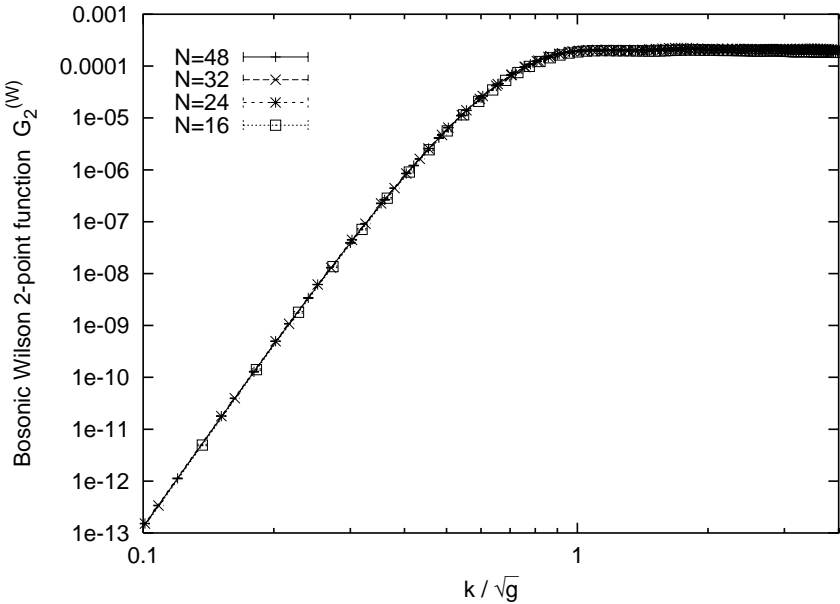


**Figure 14:** The bosonic Wilson 2-point function  $G_2^{(W)}$ , multiplied by  $Z^2 \propto N^2$ , plotted against  $k/\sqrt{g}$ .

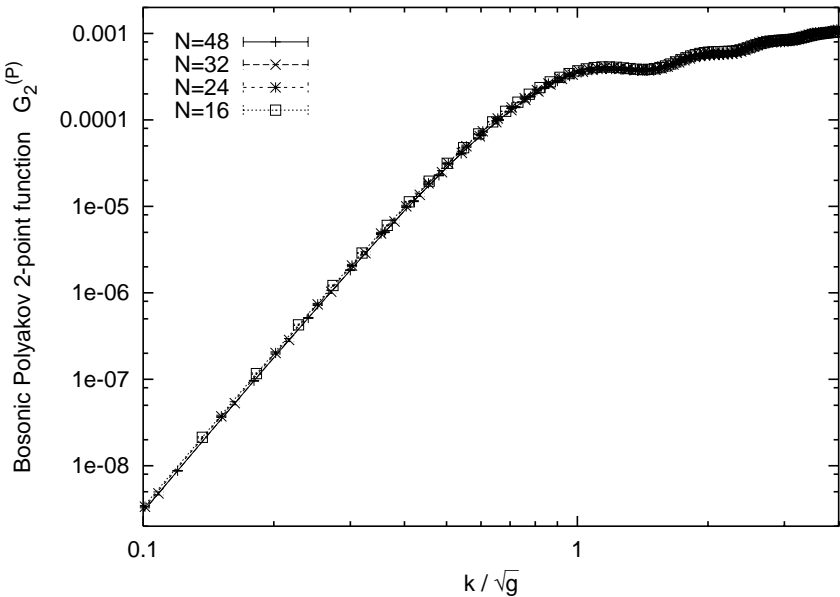


**Figure 15:** The bosonic Polyakov 2-point function  $G_2^{(P)}$ , multiplied by  $Z^2 \propto N^2$ , plotted against  $k/\sqrt{g}$ .

The data scale nicely in agreement with the theoretical prediction for large  $N$  given by eq. (4.3). For comparison we also show the 3-point and the 4-point Wilson loop correlators with the renormalization factors, which were used successfully in section 4 for the supersymmetric case. We see very clearly that the bosonic prediction is the correct one in this case.

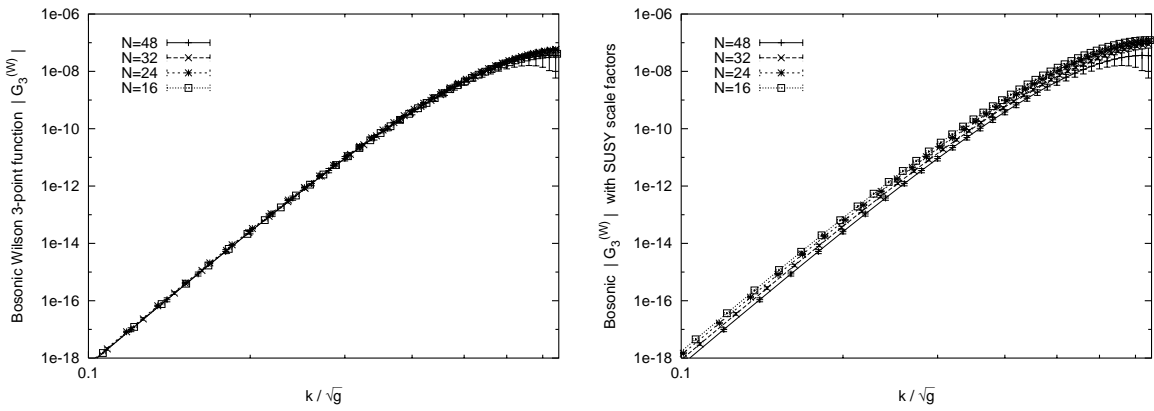


**Figure 16:** The bosonic Wilson 3-point function  $G_3^{(W)}$ , multiplied by  $Z^3 \propto N^4$ , plotted against  $k/\sqrt{g}$  on the left. On the right we show the corresponding plot using the SUSY prediction  $Z^3 \propto N^3$  instead, which leads to an inferior level of scaling.

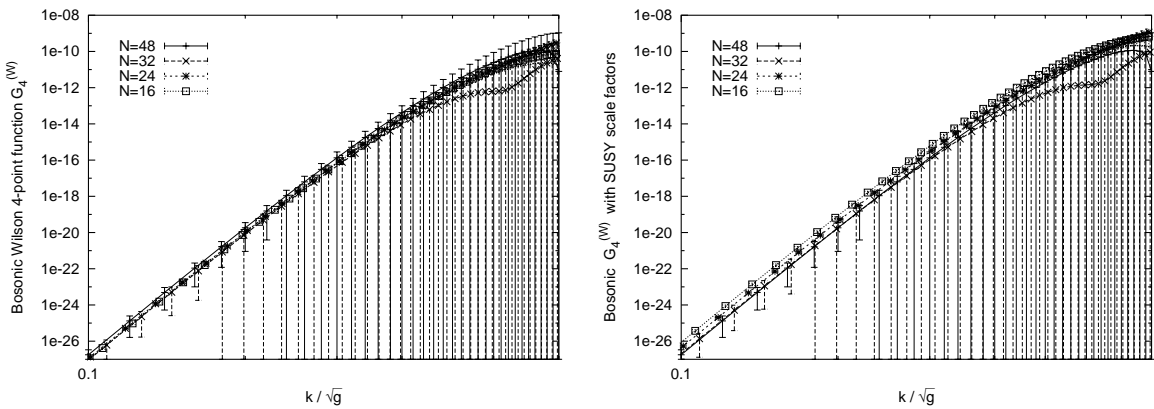


**Figure 17:** The bosonic Wilson 4-point function  $G_4^{(W)}$ , multiplied by  $Z^4 \propto N^6$ , plotted against  $k/\sqrt{g}$  on the left. On the right we show the corresponding plot using the SUSY prediction  $Z^4 \propto N^4$  instead, which leads to an inferior level of scaling.

## References

- [1] T. Banks, W. Fischler, S.H. Shenker and L. Susskind, *M-theory as a matrix model: a conjecture*, *Phys. Rev.* **D 55** (1997) 5112 [[hep-th/9610043](#)].
- [2] N. Ishibashi, H. Kawai, Y. Kitazawa and A. Tsuchiya, *A large- $N$  reduced model as superstring*, *Nucl. Phys.* **B 498** (1997) 467 [[hep-th/9612115](#)].
- [3] R. Dijkgraaf, E. Verlinde and H. Verlinde, *Matrix string theory*, *Nucl. Phys.* **B 500** (1997) 43 [[hep-th/9703030](#)];  
V. Periwal, *Matrices on a point as the theory of everything*, *Phys. Rev.* **D 55** (1997) 1711 [[hep-th/9611103](#)];  
T. Yoneya, *Schild action and space-time uncertainty principle in string theory*, *Prog. Theor. Phys.* **97** (1997) 949 [[hep-th/9703078](#)];

- J. Polchinski, *M-theory and the light cone*, *Prog. Theor. Phys. Suppl.* **134** (1999) 158 [[hep-th/9903165](#)];  
 H. Sugawara, *F- and M-theories as gauge theories of area preserving algebra*, [hep-th/9708029](#);  
 H. Itoyama and A. Tokura, *USp(2k) matrix model: F-theory connection*, *Prog. Theor. Phys.* **99** (1998) 129 [[hep-th/9708123](#)]; *USp(2k) matrix model: non-perturbative approach to orientifolds*, *Phys. Rev. D* **58** (1998) 026002 [[hep-th/9801084](#)];  
 K. Ezawa, Y. Matsuo and K. Murakami, *Matrix model for Dirichlet open string*, *Phys. Lett. B* **439** (1998) 29 [[hep-th/9802164](#)].
- [4] N. Kim and S.-J. Rey, *M(atrix) theory on an orbifold and twisted membrane*, *Nucl. Phys. B* **504** (1997) 189 [[hep-th/9701139](#)];  
 T. Banks and L. Motl, *Heterotic strings from matrices*, *J. High Energy Phys.* **12** (1997) 004 [[hep-th/9703218](#)];  
 D.A. Lowe, *Heterotic M(atrix) string theory*, *Phys. Lett. B* **403** (1997) 243 [[hep-th/9704041](#)];  
 S.-J. Rey, *Heterotic M(atrix) strings and their interactions*, *Nucl. Phys. B* **502** (1997) 170 [[hep-th/9704158](#)];  
 P. Hořava, *Matrix theory and heterotic strings on tori*, *Nucl. Phys. B* **505** (1997) 84 [[hep-th/9705055](#)];  
 M. Krogh, *A matrix model for heterotic Spin(32)/ $\mathbb{Z}_2$  and type-I string theory*, *Nucl. Phys. B* **541** (1999) 87 [[hep-th/9801034](#)];  
 M. Krogh, *Heterotic matrix theory with Wilson lines on the lightlike circle*, *Nucl. Phys. B* **541** (1999) 98 [[hep-th/9803088](#)].
- [5] D. Bigatti and L. Susskind, *Review of matrix theory*, [hep-th/9712072](#);  
 T. Banks, *TASI lectures on matrix theory*, [hep-th/9911068](#);  
 A. Bilal, *M(atrix) theory: a pedagogical introduction*, *Fortsch. Phys.* **47** (1999) 5 [[hep-th/9710136](#)];  
 W. Taylor IV, *The M(atrix) model of M-theory*, [hep-th/0002016](#).
- [6] H. Aoki, S. Iso, H. Kawai, Y. Kitazawa, A. Tsuchiya and T. Tada, *IIB matrix model*, *Prog. Theor. Phys. Suppl.* **134** (1999) 47 [[hep-th/9908038](#)].
- [7] T. Eguchi and H. Kawai, *Reduction of dynamical degrees of freedom in the large-N gauge theory*, *Phys. Rev. Lett.* **48** (1982) 1063.
- [8] M. Fukuma, H. Kawai, Y. Kitazawa and A. Tsuchiya, *String field theory from IIB matrix model*, *Nucl. Phys. B* **510** (1998) 158 [[hep-th/9705128](#)].
- [9] A. Fayyazuddin, Y. Makeenko, P. Olesen, D.J. Smith and K. Zarembo, *Towards a non-perturbative formulation of IIB superstrings by matrix models*, *Nucl. Phys. B* **499** (1997) 159 [[hep-th/9703038](#)];  
 C.F. Kristjansen and P. Olesen, *A possible IIB superstring matrix model with Euler characteristic and a double scaling limit*, *Phys. Lett. B* **405** (1997) 45 [[hep-th/9704017](#)];

- J. Ambjørn and L. Chekhov, *The NBI matrix model of IIB superstrings*, *J. High Energy Phys.* **12** (1998) 007 [[hep-th/9805212](#)];  
 S. Hirano and M. Kato, *Prog. Theor. Phys.* **98** (1997) 1371;  
 I. Oda, *Background independent matrix models*, *Phys. Lett. B* **427** (1998) 267 [[hep-th/9801051](#)];  
 N. Kitsunezaki and J. Nishimura, *Unitary IIB matrix model and the dynamical generation of the space time*, *Nucl. Phys. B* **526** (1998) 351 [[hep-th/9707162](#)];  
 T. Tada and A. Tsuchiya, *On the supersymmetric formulation of unitary matrix model of type-IIB*, [hep-th/9903037](#);  
 S. Oda and T. Yukawa, *Type-IIB random superstrings*, *Prog. Theor. Phys.* **102** (1999) 215 [[hep-th/9903216](#)].
- [10] T. Nakajima and J. Nishimura, *Numerical study of the double scaling limit in two-dimensional large- $N$  reduced model*, *Nucl. Phys. B* **528** (1998) 355 [[hep-th/9802082](#)].
- [11] J. Ambjørn, Y.M. Makeenko, J. Nishimura and R.J. Szabo, *Finite  $N$  matrix models of noncommutative gauge theory*, *J. High Energy Phys.* **11** (1999) 029 [[hep-th/9911041](#)]; *Nonperturbative dynamics of noncommutative gauge theory*, *Phys. Lett. B* **480** (2000) 399 [[hep-th/0002158](#)]; *Lattice gauge fields and discrete noncommutative Yang-Mills theory*, *J. High Energy Phys.* **05** (2000) 023 [[hep-th/0004147](#)].
- [12] W. Krauth and M. Staudacher, *Finite Yang-Mills integrals*, *Phys. Lett. B* **435** (1998) 350 [[hep-th/9804199](#)].
- [13] T. Hotta, J. Nishimura and A. Tsuchiya, *Dynamical aspects of large- $N$  reduced models*, *Nucl. Phys. B* **545** (1999) 543 [[hep-th/9811220](#)].
- [14] W. Krauth, H. Nicolai and M. Staudacher, *Monte Carlo approach to M-theory*, *Phys. Lett. B* **431** (1998) 31 [[hep-th/9803117](#)].
- [15] W. Krauth and M. Staudacher, *Eigenvalue distributions in Yang-Mills integrals*, *Phys. Lett. B* **453** (1999) 253 [[hep-th/9902113](#)].
- [16] W. Krauth, J. Plefka and M. Staudacher, *Yang-Mills integrals*, *Class. and Quant. Grav.* **17** (2000) 1171 [[hep-th/9911170](#)].
- [17] J. Hoppe, V. Kazakov and I.K. Kostov, *Dimensionally reduced SYM<sub>4</sub> as solvable matrix quantum mechanics*, *Nucl. Phys. B* **571** (2000) 479 [[hep-th/9907058](#)].
- [18] S. Gottlieb, W. Liu, D. Toussaint, R.L. Renken and R.L. Sugar, *Hybrid molecular dynamics algorithms for the numerical simulation of quantum chromodynamics*, *Phys. Rev. D* **35** (1987) 2531.
- [19] H. Aoki, S. Iso, H. Kawai, Y. Kitazawa and T. Tada, *Space-time structures from IIB matrix model*, *Prog. Theor. Phys.* **99** (1998) 713 [[hep-th/9802085](#)].
- [20] S. Iso and H. Kawai, *Space-time and matter in IIB matrix model: gauge symmetry and diffeomorphism*, *Int. J. Mod. Phys. A* **15** (2000) 651 [[hep-th/9903217](#)].

- [21] T. Yoneya, in *Wandering in the fields*, K. Kawarabayashi and A. Ukawa eds., World Scientific, 1987, p. 419; in *Quantum string theory*, N. Kawamoto and T. Kugo eds., Springer, 1988, p. 23; *On the interpretation of minimal length in string theories*, *Mod. Phys. Lett. A* **4** (1989) 1587.
- [22] G. Bhanot, U.M. Heller and H. Neuberger, *The quenched Eguchi-Kawai model*, *Phys. Lett. B* **113** (1982) 47.
- [23] G. Parisi, *A simple expression for planar field theories*, *Phys. Lett. B* **112** (1982) 463.
- [24] D.J. Gross and Y. Kitazawa, *A quenched momentum prescription for large- $N$  theories*, *Nucl. Phys. B* **206** (1982) 440.
- [25] S.R. Das and S.R. Wadia, *Translation invariance and a reduced model for summing planar diagrams in QCD*, *Phys. Lett. B* **117** (1982) 228.
- [26] J. Greensite and M.B. Halpern, *Quenched master fields*, *Nucl. Phys. B* **211** (1983) 343;  
J. Alfaro and B. Sakita, *Derivation of quenched momentum prescription by means of stochastic quantization*, *Phys. Lett. B* **121** (1983) 339.
- [27] R.L. Mkrtchyan and S.B. Khokhlachëv, *Sov. Phys. JETP Lett.* **37** (1983) 193.
- [28] T. Suyama and A. Tsuchiya, *Exact results in  $N_c = 2$  IIB matrix model*, *Prog. Theor. Phys.* **99** (1998) 321 [[hep-th/9711073](#)].
- [29] E. Brézin and V.A. Kazakov, *Exactly solvable field theories of closed strings*, *Phys. Lett. B* **236** (1990) 144;  
M.R. Douglas and S.H. Shenker, *Strings in less than one-dimension*, *Nucl. Phys. B* **335** (1990) 635;  
D.J. Gross and A.A. Migdal, *Non-perturbative two-dimensional quantum gravity*, *Phys. Rev. Lett.* **64** (1990) 127.
- [30] J. Ambjørn and S. Varsted, *Dynamical triangulated fermionic surfaces*, *Phys. Lett. B* **257** (1991) 305.
- [31] J. Ambjørn, L. Chekhov, C.F. Kristjansen and Y. Makeenko, *Matrix model calculations beyond the spherical limit*, *Nucl. Phys. B* **404** (1993) 127 [[hep-th/9302014](#)];  
J. Ambjørn, B. Durhuus and T. Jonsson, *Quantum geometry* sections 4.3 and 4.4, Cambridge Monographs, 1997.
- [32] S.D. H. Hsu, *Gaugino determinant in supersymmetric Yang-Mills theory*, *Mod. Phys. Lett. A* **13** (1998) 673 [[hep-th/9704149](#)].
- [33] D. Weingarten, *Monte Carlo algorithms for QCD*, *Nucl. Phys. B* **9** (*Proc. Suppl.*) (1989) 447.

- [34] D.J. E. Callaway and A. Rahman, *The microcanonical ensemble: a new formulation of lattice gauge theory*, *Phys. Rev. Lett.* **49** (1982) 613;  
J. Polonyi and H.W. Wyld, *Microcanonical simulation of fermionic systems*, *Phys. Rev. Lett.* **51** (1983) 2257.
- [35] J. Stoer and R. Bulirsch, *Introduction to numerical analysis*, New York, Springer-Verlag, 1980, chapter 8.
- [36] S. Duane, A.D. Kennedy, B.J. Pendleton and D. Roweth, *Hybrid Monte Carlo*, *Phys. Lett.* **B 195** (1987) 216.